ACS Chemical Neuroscience
Cite This: ACS Chem. Neurosci. XXXX, XXX, XXX−XXX
Research Article
pubs.acs.org/chemneuro

# Identification and Structure−Activity Relationship Study of Imidazo[1,2-*a*]pyridine-3-amines as First Selective Inhibitors of Excitatory Amino Acid Transporter Subtype 3 (EAAT3)

Peng Wu, Walden E. Bjørn-Yoshimoto, Markus Staudt, Anders A. Jensen,* and Lennart Bunch*

Department of Drug Design and Pharmacology, Faculty of Health and Medical Sciences, University of Copenhagen, Copenhagen DK-2100, Denmark

Supporting Information

**ABSTRACT:** In the present study, screening of a library of 49,087 compounds at the excitatory amino acid transporter subtype 3 (EAAT3) led to the identification of 2-(furan-2-yl)-8-methyl-*N*-(*o*-tolyl)imidazo[1,2-*a*]pyridin-3-amine (**3a**) which showed a >20-fold preference for inhibition of EAAT3 ($IC_{50}$ = 13 $\mu$M) over EAAT1,2,4 (EAAT1: $IC_{50}$ ∼ 250 $\mu$M; EAAT2,4: $IC_{50}$ > 250 $\mu$M). It was shown that a small lipophilic substituent (methyl or bromine) at the 7- and/or 8-position was essential for activity. Furthermore, the substitution pattern of the *o*-tolyl group (compound **5b**) and the chemical nature of the substituent in the 2-position (compound **7b**) were shown to be essential for the selectivity toward EAAT3 over EAAT1,2. The most prominent analogues to come out of this study are **3a** and **3e** that display ∼35-fold selectivity for EAAT3 ($IC_{50}$ = 7.2 $\mu$M) over EAAT1,2,4 ($IC_{50}$ ∼ 250 $\mu$M).

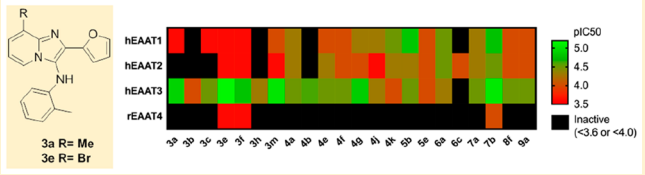


**KEYWORDS:** *Glutamate, excitatory amino acid transporter, EAAT3, EAAT3 inhibitors*

## INTRODUCTION

(*S*)-Glutamate (Glu) is the major excitatory neurotransmitter in the mammalian central nervous system (CNS), where it is central for essentially all physiological and pathophysiological processes. The synaptic reuptake of Glu is governed by a family of excitatory amino acid transporters (EAATs), which thus function as key regulators of glutamatergic transmission.[1−7] Since dysfunction in the glutamatergic system is implicated in numerous neurological and psychiatric disorders, and since therapeutic intervention in several other disorders via glutamatergic mechanisms also has been proposed, there is a considerable therapeutic potential in ligands modulating Glu transport.[2,4,7−10]

The five EAAT subtypes (EAAT1−5) are differentially expressed at the cellular level and throughout the CNS. EAAT1,2 and EAAT3,4,5 are predominantly expressed in glia cells and in neurons, respectively, and while EAAT1,2,3 are abundantly expressed throughout the brain, EAAT4 and EAAT5 are almost exclusively localized in the cerebellum and retina, respectively.[1,3,7] As the EAAT are responsible for the vast majority of Glu uptake in the CNS,[1] the EAAT2 subtype is the main transporter of interest when it comes to the hyperactivity in the glutamatergic system and the neurotoxic processes associated with various neurological and neurodegenerative disorders.[1,3,8,9,11] However, the minor EAAT subtypes also mediate important physiological functions, and in light of the more discrete expression and specialized functions of these EAATs compared to the key importance of EAAT2 for overall Glu uptake they could hold advantages in terms of being suitable drug targets.[1−3,12] For example, the predominant neuronal EAAT subtype, EAAT3, contributes significantly to glutamatergic transmission as a synaptic buffer regulating the clearance of Glu from active synapses,[13,14] and EAAT3 internalization has been found to be a key component of the augmented glutamatergic signaling underlying the psychostimulant effects of amphetamine.[12,15,16] In addition to its role for synaptic Glu clearance, EAAT3-mediated Glu and cysteine uptake has been reported to be important for GABAergic neurotransmission[17−19] and for glutathione synthesis in neurons,[20−23] respectively, and the transporter also seems to play a role in chronic pain[24] with its expression being dynamically regulated by chronic opioid treatment.[25−27] EAAT3 has been also been implicated in several pathological states, most compellingly when it comes to amino aciduria where reduced cellular uptake of Glu and aspartate results in increased renal excretion of the amino acids,[28] but increasing evidence is also indicative of a role for EAAT3 in psychiatric disorders such as obsessive compulsive disorder[16,29−32] and schizophrenia.[33,34] However, the exact contributions of EAAT3 to mechanisms underlying these physiological functions and pathophysiological conditions are still quite unclear, and conflicting observations have often been reported in different studies of these functions. Thus, while the literature certainly substantiates the therapeutic potential of EAAT3, it also underlines the need for better pharmacological tools to explore and exploit this potential further.[12,16]

**Received:** August 13, 2019
**Accepted:** September 17, 2019






DOI: 10.1021/acschemneuro.9b00447
ACS Chem. Neurosci. XXXX, XXX, XXX−XXX

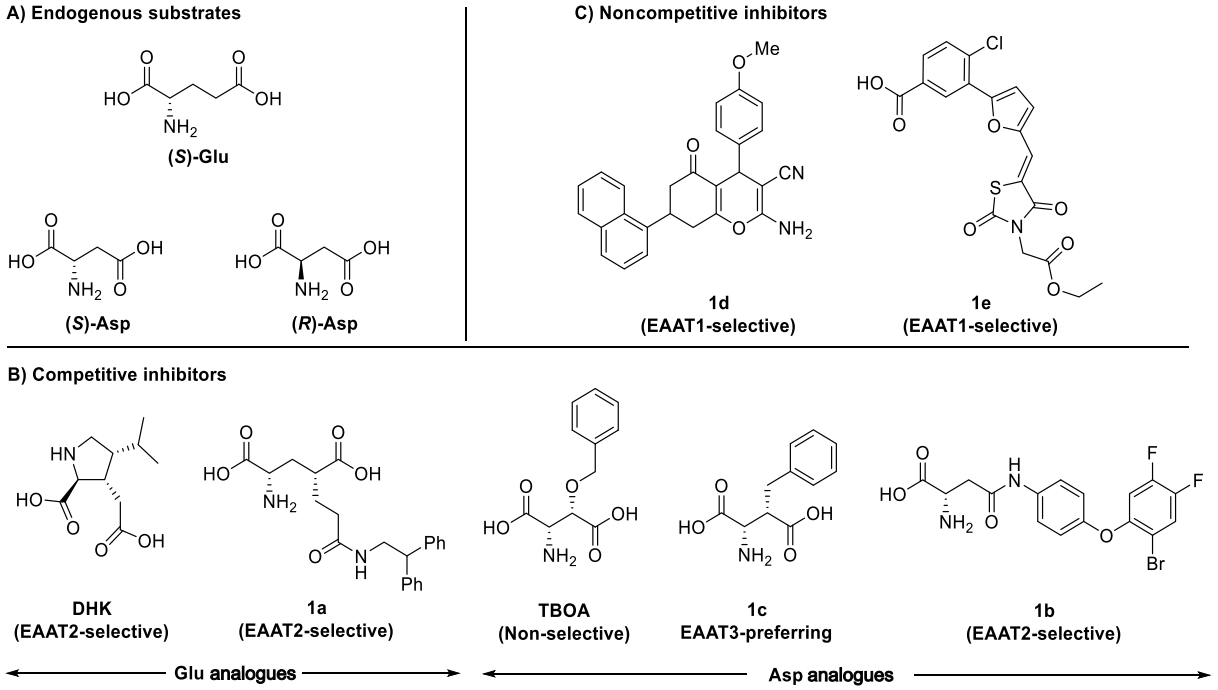


**Figure 1.** Chemical structures: (A) Endogenous EAAT substrates (*S*)-Glu, (*S*)-Asp, and (*R*)-Asp. (B) Competitive EAAT inhibitors TBOA,[12] DHK,[14,15] **1a**,[16] **1b**,[17] and **1c**.[25] (C) Noncompetitive EAAT1 inhibitors **1d**[21] and **1e**.[24]

In contrast to decades of intensive research on therapeutics in the fields of ionotropic and metabotropic Glu receptors,[35,36] the EAATs have attracted considerably less attention as drug targets over the years, which means that explorations into the physiological roles of and the therapeutic potential in the transporters still are hampered by the lack of pharmacological tools.[2,4] Most EAAT ligands reported to date are amino acids developed using the endogenous EAAT substrates (*S*)-Glu, (*S*)-aspartate, and (*R*)-aspartate as leads (Figure 1).[4] This approach has resulted in the identification of EAAT2-selective inhibitors, including the conformationally restricted Glu analogue dihydrokainic acid (DHK), the 4-substituted Glu analogue (2*S*,4*R*)-2-amino-4-(3-(2,2-diphenylethylamino)-3-oxopropyl)-pentanedioic acid (**1a**), and the functionalized asparagine analogue *N*-[4-(2-bromo-4,5-difluorophenoxy)phenyl]-L-asparagine (WAY-213613, **1b**) (Figure 1).[37−40] However, selective ligands for other EAAT subtypes have not emerged from these efforts, and thus, the most EAAT3-selective ligand reported to date, L-*threo*-*β*-benzylaspartate (L-*β*-BA, **1c**, Figure 1), only exhibits 4−10-fold higher inhibitory potency at EAAT3 than at other EAATs.[41,42] In our continued search for novel pharmacological tools applicable for studies of the physiological functions governed by EAATs, we have previously applied screenings of small commercial compound libraries. This approach has led to the development two structurally novel series of highly EAAT1-selective inhibitors, represented by UCPH-101 (**1d**) and compound **1e** (Figure 1).[43−45] In the present study, we report the discovery of the first class of EAAT3-selective inhibitors based on a hit identified from screening of an ∼50,000 compound library at EAAT3 followed by an elaborate structure−activity relationship (SAR) study.

## RESULTS AND DISCUSSION

**Identification of a Novel EAAT3-Selective Inhibitor.** In search for novel lead structures which display EAAT activity and in particular for EAAT3-selective modulators, screening of a ∼50,000 compound library at EAAT3 was performed (see further description of the compound library in Methods). The screening was performed using a stable hEAAT3-HEK293 cell line[39] in the FLIPR Membrane Potential Blue (FMP) assay, where the membrane potential changes in the cells arising from the electrogenic transport process of the EAAT are measured by use of a fluorescent dye.[39] The compounds were screened for modulatory activity at the transporter at an assay concentration of ∼25 $\mu$M or 5 mg/mL using Glu at an $EC_{80}$ ($EC_{70}$−$EC_{90}$) concentration as EAAT substrate.

The screening identified compound **3a** (2-(furan-2-yl)-8-methyl-*N*-(*o*-tolyl)imadazo[1,2-*a*]pyridine-3-amine) to inhibit the Glu-induced response in the hEAAT3-HEK293 cells significantly (Figure 2A). After confirmation of its inhibitory EAAT3 activity, **3a** was found not to modulate GABA-evoked signaling through a HEK293 cell line expressing the human h$\rho$1 $GABA_AR$[46] in the FMP assay, demonstrating that the effects of **3a** on the Glu-induced response in the hEAAT3-HEK293 cells was indeed mediated via the EAAT3 transporter (data not shown).

The EAAT3 inhibitory activity of **3a** was verified and its selectivity profile across the EAAT family was determined in a conventional [$^3$H]-D-aspartate ([$^3$H]-D-Asp) uptake assay using stable hEAAT1-, hEAAT2-, and hEAAT3-HEK293 and rEAAT4-tsA201 cell lines.[39,47] In this assay, **3a** displayed $IC_{50}$ values of ∼250 $\mu$M, >250 $\mu$M, 13 $\mu$M, and >250 $\mu$M in hEAAT1, hEAAT2, hEAAT3, and rEAAT4, respectively, thus displaying ∼20-, >20-, and >20-fold selectivity as an inhibitor of hEAAT3 over hEAAT1, hEAAT2, and rEAAT4, respectively (Figure 2B, Tables 1−8).

**Design and Synthesis of 3a Analogues.** The fused imidazole bridgehead nitrogen heterocyclic core found in compound **3a** is readily synthesized from the three-component Groebke−Blackburn−Bienaymé (GBB) reaction (Scheme 1).[48−51] Thus, by variation of the substituents on the amidine, aldehyde, and isocyanide components, a large number of


DOI: 10.1021/acschemneuro.9b00447
ACS Chem. Neurosci. XXXX, XXX, XXX−XXX

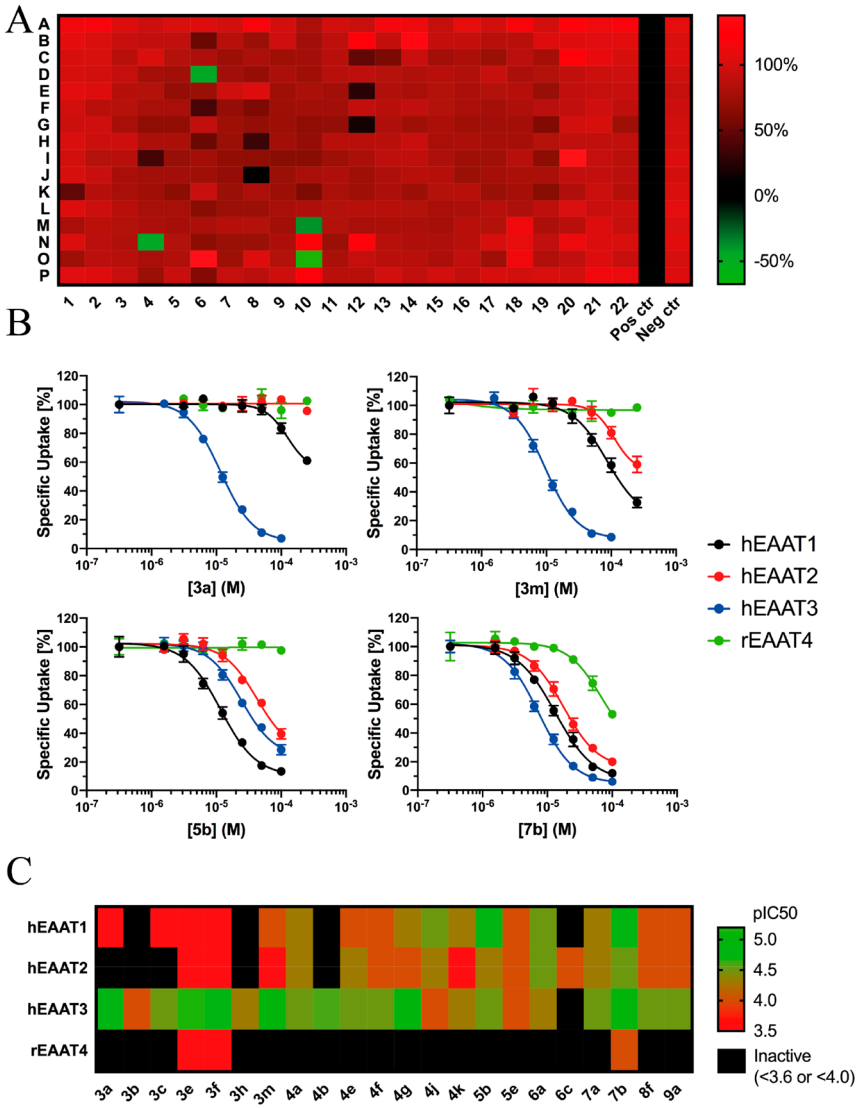


**Figure 2.** Functional properties of selected analogues from the series of EAAT3-selective inhibitors. (A) Heat map of data obtained for the plate containing hit compound **3a** (2-(furan-2-yl)-8-methyl-*N*-(*o*-tolyl)imidazo[1,2-*a*]pyridin-3-amine; well N04) in the compound library screening in the hEAAT3-HEK293 cell line in the FMP assay. The wells in columns 23 and 24 contain positive controls (Pos ctr; buffer containing 0.025% DMSO) and negative controls (Neg ctr; buffer containing 0.025% DMSO and 300 $\mu$M L-Glu), respectively. The data is given as percentage of the span between the values obtained for the positive and negative controls. (B) Representative concentration−inhibition curves for **3a**, **3m**, **5b**, and **7b** at the hEAAT1-HEK293 (black), hEAAT2-HEK293 (red), hEAAT3-HEK293 (blue), and rEAAT4-tsA201 (green) cell lines in the [$^3$H]-D-Asp uptake assay. Data are from representative individual experiments and are given as mean ± SD values in % of specific [$^3$H]-D-Asp uptake. (C) Heat map of the selectivity profiles displayed by selected (active) compounds at EAAT1−4. The coloring is given based on mean $pIC_{50}$ values exhibited by the compounds at the four transporters in the [$^3$H]-D-Asp uptake assay, with black indicating that the compound either were completely inactive at the specific transporter or inhibited specific [$^3$H]-D-Asp uptake through it significantly less than 50% at the highest concentration tested (>100 or >250 $\mu$M).

**Scheme 1. Three-Component (Amidine 11, Aldehyde 12, and Isocyanide 13) Groebke−Blackburn−Bienaymé Reaction for the Synthesis of the Imidazo[1,2-*a*]pyridin-3-amine Core, Series 3−10**

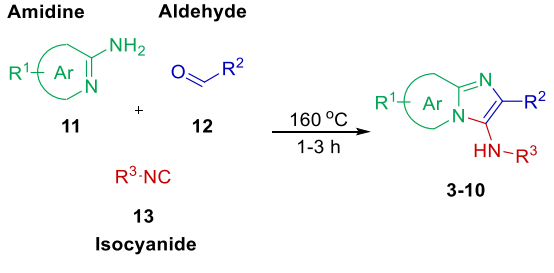


analogues of **3a** can easily be accessed. A total of 89 analogues of **3a** were obtained by in house synthesis or purchased from commercial suppliers and included in the present SAR study (Figure 3).

The effect on EAAT3 inhibition of varying the substituent(s) on the pyridine ring was explored by employing different amidines (series 3, Figure 3) (Table 1). Substitutions on or replacement of the furan ring at the 2-position of the imidazopyridine core was achieved by employing different aromatic and aliphatic aldehydes (series 4, Figure 3) (Table 2), and the 3-amine handle was formed by using corresponding isocyanides (series 5, Figure 3) (Table 3). Combinations of the above variations gave access to analogues with simultaneous variations at two points (Tables 4−6) or three points (Table 7).



DOI: 10.1021/acschemneuro.9b00447
ACS Chem. Neurosci. XXXX, XXX, XXX−XXX

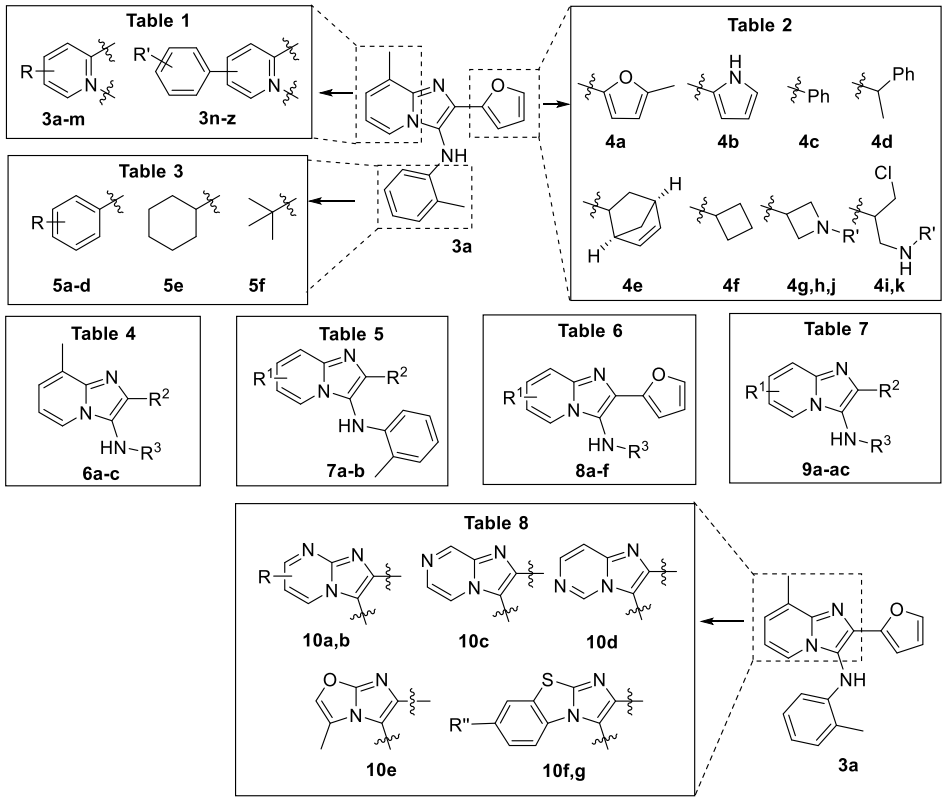


**Figure 3.** Overview of compounds series **3**−**10** included in the SAR study and the chemical modifications introduced into **3a** in the different analogues. The tables outlining the pharmacological data of the different compound series are indicated.

The bicyclic imidazo[1,2-*a*]pyridine scaffold core was replaced by other aromatic bi- or tricyclic scaffolds (Table 8).

*Synthesis of Series **3**−**10**.* The target compounds with a bicyclic imidazo[1,2-*a*]pyridin-3-amine scaffold were synthesized via GBB reaction, which was performed in a highly efficient manner under solvent- and catalyst-free conditions (Scheme 2).[48] Readily available amidine, aldehyde, and isocyanide substrates were subjected to this three-component transformation at 160 °C for 1−3 h to afford target compounds **3a**−**g**, **3i**−**m**, **4b**−**g**, **5d**−**f**, **6c**, **7b**, **8a**−**8e**, and **10a**−**10g**) in yields up to 98%, without further optimization. For the GBB products **3e**−**g** comprising a bromo substituent at the 6-, 7-, or 8-position of the imidazo[1,2-*a*]pyridin-3-amine scaffold, a following Suzuki-coupling reaction was performed to give compounds **3n**−**z** in good to excellent yields up to 99% using 5 mol % XPhos-Pd-G3 catalyst under microwave irradiation at 100 °C for 45 min. For the GBB reaction product **4g** with a Boc-protected azetidine moiety at the 2-position of the imidazo[1,2-*a*]pyridin-3-amine scaffold, a Boc-deprotection step in acidic condition followed by an acetylation reaction using acetyl chloride gave both azetidine-acetylated products **4h** and side product **4i**, formed through ring-opening of the azetidine moiety by chloride, in a combined yield of 71%. Replacement of the acetyl chloride with 2-fluorobenzoyl chloride gave **4j** and **4k** in a combined yield of 77%.

*Structure−Activity Relationship of **3a** Analogues as EAAT Inhibitors.* The functional properties of all 89 analogues of **3a** (series **3**−**10**) were characterized at stable hEAAT1-, hEAAT2-, and hEAAT3-HEK293 and rEAAT4-tsA201 cell lines in the [$^3$H]-D-Asp uptake assay. (S)-Glu and **3a** were tested as controls in all rounds of testing. The functional properties of the analogues are given in Figure 3 and Tables 1−8.[52]

In compound series **3**, we evaluated the impact of different substituents on the pyridine moiety of the bicyclic scaffold core on EAAT1−4 activity (Table 1). The analogues were obtained by applying appropriately substituted 2-aminopyridines **11** in the synthesis. First, with removal of the 8-methyl group, compound **3b** (R = H) resulted in a 10-fold loss of inhibitory potency at EAAT3. Next, repositioning of the 8-methyl group of **3a** to the 7-position (**3c**) and the 6-position (**3d**) reduced the inhibitory potency of the lead at EAAT3 slightly and significantly, respectively. The EAAT3 inhibitory potency was slightly improved when the 8-methyl group was replaced with a bromine, compound **3e** ($IC_{50}$ = 7.2 $\mu$M), conserved upon substituting the 7-methyl group with a bromine, compound **3f**, whereas the 6-bromo analogue **3g** was inactive. Finally, the 6-Cl analogue **3h** displayed only moderate effect at EAAT3 (Table 1). Introduction of other substituents at the 8-position, both electron-donating and electron-withdrawing groups, led to compounds without activity or with negligible activity at EAAT3 (**3i**−**k**). While the 8-methyl-6-chloro analogue **3l** was inactive, the 8-bromo-7-methyl analogue **3m** was equipotent to **3a**, displaying $IC_{50}$ values of 9.6 $\mu$M at EAAT3, ∼100 $\mu$M at EAAT1, and >250 $\mu$M at EAAT2,4 (Figure 2B, Table 1). Analogues **3n**−**z**, in which (un)substituted phenyl rings were incorporated in the 6-, 7-, or 8-positions, were all inactive ($IC_{50}$ > 250 $\mu$M) at EAAT3.

All in all, these data showed that a small lipophilic substituent in the 8- and/or 7-positions (compounds **3a**,**c**,**e**,**f**) is of key importance for the observed EAAT3 inhibitory potency of this compound class. Finally, with the exception of the moderate EAAT1 activity displayed by **3m** ($IC_{50}$ ∼ 100 $\mu$M), all compounds in this series (**3a**−**z**) either displayed negligible activity or were completely inactive at EAAT1,2,4 at


DOI: 10.1021/acschemneuro.9b00447
ACS Chem. Neurosci. XXXX, XXX, XXX−XXX

**Scheme 2. Synthesis of Representative Compounds 3a, 3e, 3p, and 4g−k**

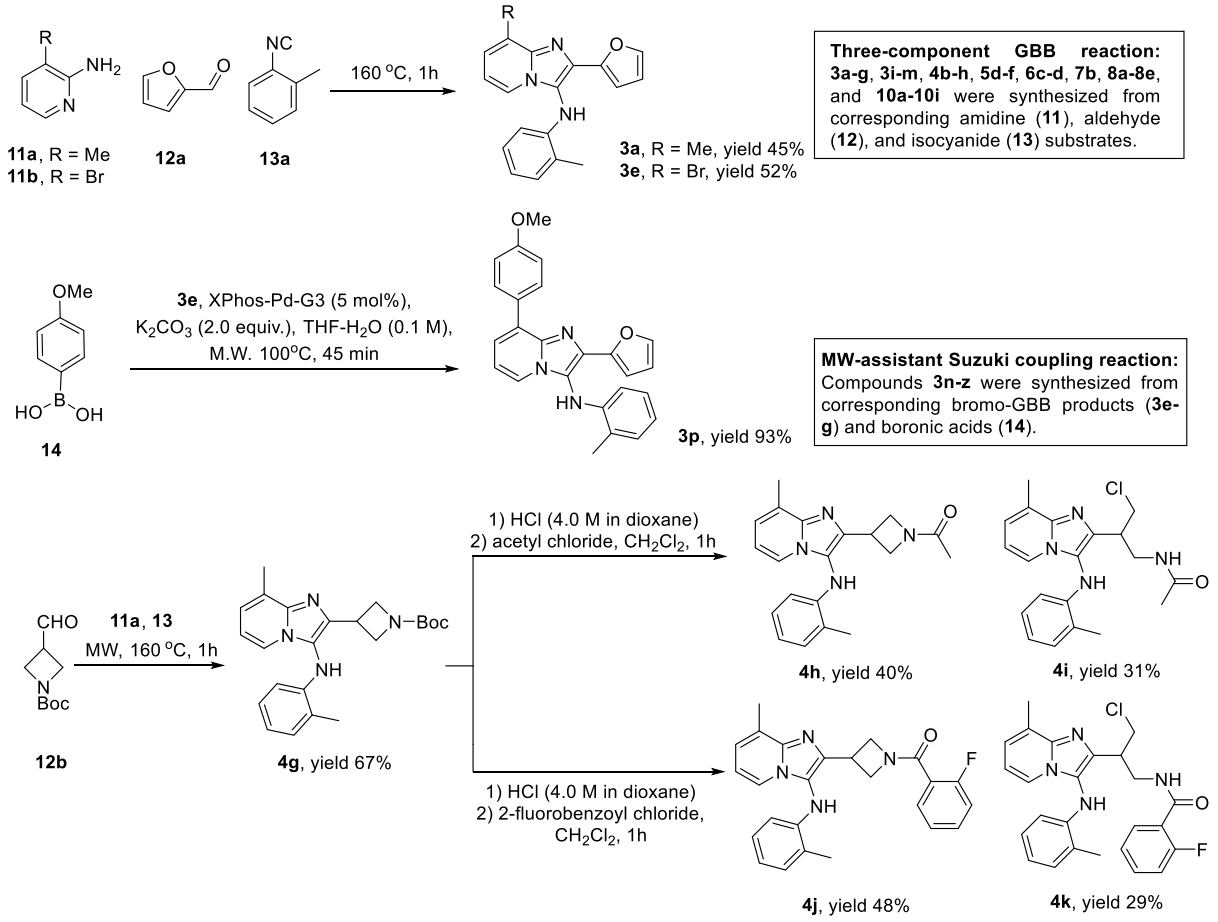


concentrations up to 250 $\mu$M. Most notably, **3e**, the most potent EAAT3-inhibitor in the series, exhibited an EAAT3-over-EAAT1,2,4 selectivity ratio of ∼35-fold, and **3a** displayed ∼20-, >20-, and >20-fold selectivity for EAAT3 over EAAT1, EAAT2, and EAAT4, respectively.

In the next series, we probed the contribution of the 2-(furan-2-yl) substituent on the imidazopyridine core of **3a** for its EAAT3 activity (Table 2). Interestingly, addition of a methyl group at the 5′-position in the furan-2-yl moiety yielded a compound that exhibited equipotent, albeit moderate, inhibition at EAAT1−3 (**4a**). Replacement of the furan-2-yl moiety with a pyrrol-2-yl moiety reduced the inhibitory potency at EAAT3 slightly (**4b**), while the corresponding phenyl (**4c**) and 1-phenylethyl (**4d**) analogues displaying negligible EAAT3 inhibition (Table 2). The introduction of the bulky lipopohlic norbornenyl (**4e**) or cyclobutyl (**4f**) groups resulted in slightly reduced EAAT3 inhibitory potency (3-fold), whereas a Boc-azetidine group, compound **4g**, led to an $IC_{50}$ value at EAAT3 comparable to that of **3a**. In contrast to series **3**, analogues **4a,e,j** displayed roughly equipotent (weak) inhibition of EAAT1−3, while still being inactive at EAAT4 (Table 2).

Series **5** was a small series of analogues in which aromatic and aliphatic isocyanide substituents were introduced at the 3-position of the imidazopyridine core of **3a** (compounds **5a−f**, Table 3). The six analogues displayed slightly or substantially reduced inhibitory potency at EAAT3 compared to **3a**, with the phenyl analogue **5a** not surprisingly being the most active analogue of the six. Interestingly, introduction of an *i*Pr group in the 4′-position, analogue **5b**, led to loss of the EAAT3 selectivity, with this analogue displaying equipotent inhibition of EAAT1 and EAAT3 (Table 3, Figure 2B).

Series **6−8** all comprised analogues in which two moieties in the **3a** scaffold were varied at the same time: the 2-(furan-2-yl) and 3-amino substituents (**6a−6c**), the 2-moiety and the fused pyridine moiety (**7a**, **7b**), and substituents at the 3-amine and the fused pyridine group (**8a−8f**) (Tables 4−6). Analogue **6a** shared the 5-methylfuran-2-yl moiety with **4a** and displayed roughly the same functional properties as that analogue across EAAT1−4, whereas **6b,c** all were inactive at the transporters. Analogue **7b**, which combined the 8-bromo-7-methyl substitution pattern at the imidazopyridine core of **3m** and the Boc-azetidine from compound **4g** exhibited an interesting EAAT activity profile, displaying comparable inhibitory potency at EAAT1 and EAAT3 ($IC_{50}$ values 16 and 8.8 $\mu$M, respectively) and somewhat weaker activity at EAAT2,4 (Table 5, Figure 2B). Finally, the inactivity of analogues **8a−e** at EAAT1−4 was not surprising considering the negligible activity displayed by analogues **5e,f** that both also contains an aliphatic substituent at the 3-amino position at the imidazopyridine core. Series **9** consisted of 29 analogues that comprised modifications at all three positions (**9a−9ac**). Because of the substantial degree of variation introduced in these analogues, they were exclusively screened for activity at EAAT3, and not surprising the majority of the analogues were completely inactive at the transporter (Table 7).

Series **10** consisted of analogues wherein the imidazopyridine core of **3a** was modified or replaced (Table 8): Including an additional ring nitrogen yielded bicyclic 6-5 scaffolds imidazo-



DOI: 10.1021/acschemneuro.9b00447
ACS Chem. Neurosci. XXXX, XXX, XXX−XXX

**Table 1. SAR Study of the Importance of Substituents on the Pyridine Moiety of the Core Imidazo[1,2-*a*]pyridin-3-amine Scaffold of 3a for EAAT1−4 Activity**[c]

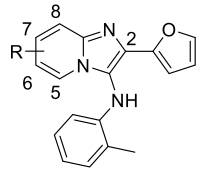


| | | $IC_{50}$ ($\mu$M) [$pIC_{50}$ ± SEM][a] | | | |
|---|---|---|---|---|---|
| compd | R | hEAAT1 | hEAAT2 | hEAAT3 | rEAAT4 |
| **3a** | 8-Me | ~250 [~3.6] | >250 [<3.6] | 13 [4.90 ± 0.02] | >250 [<3.6] |
| **3b** | H | >250 [<3.6] | >250 [<3.6] | ~100 [~4.0] | >250 [<3.6] |
| **3c** | 7-Me | ~250 [~3.6] | >250 [<3.6] | ~30 [~4.5] | >250 [<3.6] |
| **3d** | 6-Me | ~250 [~3.6] | ~250 [~3.6] | ~100 [~4.0] | ~250 [~3.6] |
| **3e** | 8-Br | ~250 [~3.6] | ~250 [~3.6] | 7.2 [5.14 ± 0.06] | ~250 [~3.6] |
| **3f** | 7-Br | ~250 [~3.6] | ~250 [~3.6] | 16 [4.80 ± 0.09] | ~250 [~3.6] |
| **3g** | 6-Br | >250 [<3.6] | >250 [<3.6] | >250 [<3.6] | >250 [<3.6] |
| **3h**[b] | 6-Cl | >250 [<3.6] | >250 [<3.6] | ~50 [~4.3] | >250 [<3.6] |
| **3i** | 8-$CF_3$ | >250 [<3.6] | >250 [<3.6] | >250 [<3.6] | >250 [<3.6] |
| **3j** | 8-CN | >250 [<3.6] | >250 [<3.6] | >250 [<3.6] | >250 [<3.6] |
| **3k** | 8-$NH_2$ | >250 [<3.6] | >250 [<3.6] | ~100 [~4.0] | >250 [<3.6] |
| **3l** | 8-Me, 6-Cl | >250 [<3.6] | >250 [<3.6] | >250 [<3.6] | >250 [<3.6] |
| **3m** | 8-Br,7-Me | ~100 [~4.0] | ~250 [~3.6] | 9.6 [5.02 ± 0.06] | >250 [<3.6] |
| **3n** | 8-Ph | >250 [<3.6] | >250 [<3.6] | >250 [<3.6] | >250 [<3.6] |
| **3o** | 7-Ph | >250 [<3.6] | >250 [<3.6] | >250 [<3.6] | >250 [<3.6] |
| **3p** | 8-(4-$MeOC_6H_4$) | >250 [<3.6] | >250 [<3.6] | >250 [<3.6] | >250 [<3.6] |
| **3q** | 7-(4-$MeOC_6H_4$) | >250 [<3.6] | >250 [<3.6] | >250 [<3.6] | >250 [<3.6] |
| **3r** | 6-(4-$MeOC_6H_4$) | >250 [<3.6] | >250 [<3.6] | >250 [<3.6] | >250 [<3.6] |
| **3s** | 8-(4-F-2-$MeOC_6H_3$) | >250 [<3.6] | >250 [<3.6] | >250 [<3.6] | >250 [<3.6] |
| **3t** | 7-(4-F-2-$MeOC_6H_3$) | >250 [<3.6] | >250 [<3.6] | >250 [<3.6] | >250 [<3.6] |
| **3u** | 6-(4-F-2-$MeOC_6H_3$) | >250 [<3.6] | >250 [<3.6] | >250 [<3.6] | >250 [<3.6] |
| **3v** | 7-(5-CN-2-$MeOC_6H_3$) | >250 [<3.6] | >250 [<3.6] | >250 [<3.6] | >250 [<3.6] |
| **3w** | 6-(5-CN-2-$MeOC_6H_3$) | >250 [<3.6] | >250 [<3.6] | >250 [<3.6] | >250 [<3.6] |
| **3x** | 7-(2-$CH_2OH$-4-$MeOC_6H_3$) | >250 [<3.6] | >250 [<3.6] | >250 [<3.6] | >250 [<3.6] |
| **3y** | 6-(2-$CH_2OH$-4-$MeOC_6H_3$) | >250 [<3.6] | >250 [<3.6] | >250 [<3.6] | >250 [<3.6] |
| **3z** | 6-(4-$CH_3CONHC_6H_4$) | >250 [<3.6] | >250 [<3.6] | >250 [<3.6] | >250 [<3.6] |

[a]Data are based on 3−4 independent experiments ($n$ = 3−4), except for the **3a** data ($n$ = 11). [b]Obtained from commercial supplier. [c]The inhibitory potencies displayed by the analogues in hEAAT1-HEK293, hEAAT2-HEK293, hEAAT3-HEK293, and rEAAT4-tsA201 cells in the [$^3$H]-D-Asp uptake assay are given.

[1,2-*a*]pyrimidines (**10a**,**b**), imidazo[1,2-*a*]pyrazine (**10c**), and imidazo[1,2-*c*]pyrimidine (**10d**). Replacement of the bicyclic 6-5 scaffold with a size-reduced bicyclic 5-5 scaffold yielded imidazo[2,1-*b*]oxazole (**10e**), and replacement of the bicyclic 6-5 scaffold with a more bulky tricyclic 6-5-5 scaffold yielded benzo[*d*]imidazo[2,1-*b*]thiazoles (**10f**,**g**). All these scaffold jumps led to complete loss of inhibitory activity at EAAT1−4 (Table 8).

In summary, the SAR study presented herein comprises 89 analogues of **3a** and leads to the conclusion that the presence of a small lipophilic substituent (Me, Br) in the 7- and/or 8-positions of the imidazo[1,2-*a*]pyridine core is important for EAAT3 inhibitory activity. The most potent analogue in the series, compound **3e**, only displays a 2-fold higher inhibitory potency compared to **3a** but it is ~35 fold selective as an inhibitor of EAAT3 over EAAT1,2,4. In comparison, **3a** only displays ~20-fold EAAT3-over-EAAT1 selectivity but since this analogue is completely inactive at both EAAT2 and EAAT4 at the highest concentration tested (due to solubility), it could potentially be more EAAT3-selective against these two subtypes than **3e**. Interestingly, minor structural modifications to **3a** occasionally yielded compounds that displayed equipotent inhibition of several EAAT subtypes, such **4a**, **5b** and **7b** (Figure 2B). This underlines that the EAAT3-selectivity displayed by **3a** and a couple other analogues in the series is rooted in the substitution pattern on the imidazo[1,2-*a*]pyridine-3-amine core, and that the scaffold thus potentially also could form the basis for the development of inhibitors with other EAAT subtype-selectivity profiles.

## CONCLUSION

In the present study we have identified a compound series of imidazo[1,2-*a*]pyridin-3-amines as the first class of EAAT3-selective inhibitors. The lead compound **3a** was identified from a high throughput screening of a library of 49,087 structurally diverse compounds followed by an elaborate SAR study of a total of 89 analogues, most of which were synthesized using the efficient solvent-free GBB reaction. The SAR study disclose both options and limitations on the introduction/exchange of substituents as well as when altering the chemical nature of core scaffold. Albeit significantly improved inhibitory potency (~2-fold) was not achieved in this round of SAR investigations, the most potent analogue, compound **3e**, displays ~35-fold higher inhibitory potency at EAAT3 compared to EAAT1,2,4,


DOI: 10.1021/acschemneuro.9b00447
ACS Chem. Neurosci. XXXX, XXX, XXX−XXX

Table 2. SAR Study of the Importance of Substituents on the Furan Moiety of 3a for EAAT1−4 Activity[d]

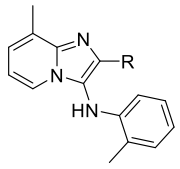

| Cpd. | R | IC50 (μM) [pIC50 ± S.E.M.][a] | | | |
|---|---|---|---|---|---|
| | | hEAAT1 | hEAAT2 | hEAAT3 | rEAAT4 |
| 4a[b] |  | ~50 [~4.3] | ~50 [~4.3] | ~30 [~4.5] | >100 [<4.0] |
| 4b |  | >250 [<3.6] | >250 [<3.6] | ~25 [~4.6] | >250 [<3.6] |
| 4c[b] |  | n.t. | n.t. | >250 [<3.6] | n.t. |
| 4d |  | ~100 [~4.0] | ~100 [~4.0] | ~250 [~3.6] | ~100 [~4.0] |
| 4e | 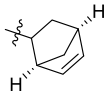 | ~100 [~4.0] | ~50 [~4.3] | ~30 [~4.5] | >250 [<3.6] |
| 4f |  | ~100 [~4.0] | ~100 [~4.0] | ~30 [~4.5] | >250 [<3.6] |
| 4g | 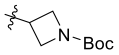 | ~50 [~4.3] | ~100 [~4.0] | 17 [4.78 ± 0.07] | >250 [<3.6] |
| 4h | 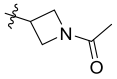 | >250 [<3.6] | >250 [<3.6] | >250 [<3.6] | >250 [<3.6] |
| 4i | 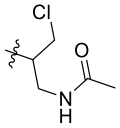 | >250 [<3.6] | >250 [<3.6] | >250 [<3.6] | >250 [<3.6] |
| 4j | 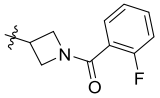 | ~50 [~4.3] | ~100 [~3.6] | ~50 [~4.3] | >250 [<3.6] |
| 4k | 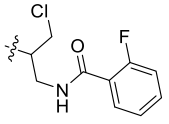 | ~30 [~4.5] | ~50 [~4.3] | ~100 [~4.0] | >250 [<3.6] |

[a]Data are based on 3−4 independent experiments ($n$ = 3−4). [b]Obtained from commercial supplier. [c]Not tested. [d]The inhibitory potencies displayed by the analogues in hEAAT1-HEK293, hEAAT2-HEK293, hEAAT3-HEK293, and rEAAT4-tsA201 cells in the [$^3$H]-D-Asp uptake assay are given.

and compounds **3a** and **3e**, as well as other analogues in the series, are considerably more EAAT3-selective than previously reported EAAT3-preferring inhibitor L-$\beta$-BA[41,42] and thus represent tool compounds for studying the physiological function and therapeutic potential of EAAT3.

## METHODS

**Chemistry.** Unless otherwise noted, reactions were performed under a nitrogen atmosphere in flame-dried glassware including microwave vials. Reagents were purchased and used as received from commercial sources or synthesized based on cited procedures.



DOI: 10.1021/acschemneuro.9b00447
ACS Chem. Neurosci. XXXX, XXX, XXX−XXX

**Table 3. SAR Study of the Importance of the 2-Methylphenyl Moiety of 3a for EAAT1−4 Activity[c]**

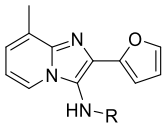

| Cpd. | R | | IC$_{50}$ (μM) [pIC$_{50}$ ± S.E.M.][a] | | | |
|---|---|---|---|---|---|---|
| | | | hEAAT1 | hEAAT2 | hEAAT3 | rEAAT4 |
| 5a[b] | | R': H | >100 [<4.0] | >100 [<4.0] | ~30 [~4.5] | >100 [<4.0] |
| 5b[b] | 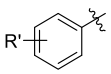 | R': 4-*i*Pr | 15 [4.82 ± 0.05] | ~50 [~4.3] | ~30 [~4.5] | >100 [<4.0] |
| 5c[b] | | R': 4-MeO | >100 [<4.0] | >100 [<4.0] | >250 [<3.6] | >100 [<4.0] |
| 5d | | R': 2,6-(Me)$_2$ | >250 [<3.6] | >250 [<3.6] | ~100 [~4.0] | >250 [<3.6] |
| 5e |  | | ~100 [~4.0] | ~100 [~4.0] | ~100 [~4.0] | >250 [<3.6] |
| 5f |  | | >250 [<3.6] | >250 [<3.6] | >250 [<3.6] | >250 [<3.6] |

[a]Data are based on 3−4 independent experiments ($n$ = 3−4). [b]Obtained from commercial supplier. [c]The inhibitory potencies displayed by the analogues in hEAAT1-HEK293, hEAAT2-HEK293, hEAAT3-HEK293, and rEAAT4-tsA201 cells in the [$^3$H]-D-Asp uptake assay are given.

**Table 4. SAR Study of the Impact of Chemical Modifications at Both the Furan and the 2-Methylphenyl Moieties of 3a on EAAT1−4 Activity[c]**

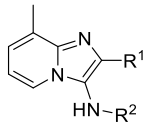

| Cpd. | R$^1$ | R$^2$ | IC$_{50}$ (μM) [pIC$_{50}$ ± S.E.M.][a] | | | |
|---|---|---|---|---|---|---|
| | | | hEAAT1 | hEAAT2 | hEAAT3 | rEAAT4 |
| 6a[b] | 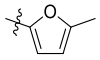 |  | ~30 [~4.5] | ~30 [~4.5] | ~50 [~4.3] | >100 [<4.0] |
| 6b[b] |  |  | n.t. | n.t. | ~100 [~4.0] | n.t. |
| 6c | 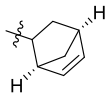 | 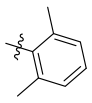 | >250 [<3.6] | ~100 [~4.0] | >250 [<3.6] | >250 [<3.6] |

[a]Data are based on 3−4 independent experiments ($n$ = 3−4). [b]Obtained from commercial supplier. n.t., not tested. [c]The inhibitory potencies displayed by the analogues in hEAAT1-HEK293, hEAAT2-HEK293, hEAAT3-HEK293, and rEAAT4-tsA201 cells in the [$^3$H]-D-Asp uptake assay are given.

Reactions were monitored by thin-layer chromatography (TLC, using Merck silica gel 60 F254 precoated plates, 0.25 mm), visualized by UV light at 254 nm. Yields refer to isolated compounds obtained by flash column chromatography (Merck 60 Å mesh, 15−40 μm) on a Buchi Reveleris Flash system, unless otherwise noted. Nuclear magnetic resonance (NMR) spectra were recorded on a Bruker 400 MHz Spectrometer ($^1$H NMR, 400 MHz; $^{13}$C NMR, 100 MHz) or a Bruker 600 MHz Spectrometer ($^1$H NMR, 600 MHz; $^{13}$C NMR, 150 MHz). NMR data were obtained in $CDCl_3$ or DMSO-$d_6$ (purchased from Cambridge Isotope Laboratories, Inc.). Chemical shifts are reported in parts per million (ppm) relative to the NMR solvent as follows: multiplicity (s = singlet, d = doublet, t = triplet, dd = double doublet,


DOI: 10.1021/acschemneuro.9b00447
ACS Chem. Neurosci. XXXX, XXX, XXX−XXX

**Table 5. SAR Study of the Impact of Chemical Modifications at Both the Furan Moiety and the Substituent on the Pyridine Moiety of 3a on EAAT1−4 Activity[c]**

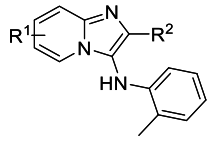

| Cpd. | $R^1$ | $R^2$ | $IC_{50}$ (μM) [$pIC_{50}$ ± S.E.M.][a] | | | |
|---|---|---|---|---|---|---|
| | | | hEAAT1 | hEAAT2 | hEAAT3 | rEAAT4 |
| **7a**[b] | H |  | ~50 [~4.3] | ~50 [~4.3] | ~30 [~4.5] | >100 [<4.0] |
| **7b** | 8-Br,7-Me | 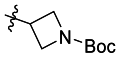 | 16 [4.79 ± 0.06] | ~30 [~4.5] | 8.8 [5.05 ± 0.05] | ~100 [~4.0] |

[a]Data are based on 3−4 independent experiments ($n$ = 3−4). [b]Obtained from commercial supplier. [c]The inhibitory potencies displayed by the analogues in hEAAT1-HEK293, hEAAT2-HEK293, hEAAT3-HEK293, and rEAAT4-tsA201 cells in the [$^3$H]-D-Asp uptake assay are given.

**Table 6. SAR Study of the Impact of Chemical Modifications at Both the Substituent on the Pyridine Moiety and the 2-Methylphenyl Moiety of 3a on EAAT1−4 Activity[c]**

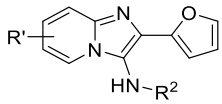

| Cpd. | $R^1$ | $R^2$ | $IC_{50}$ (μM) [$pIC_{50}$ ± S.E.M.][a] | | | |
|---|---|---|---|---|---|---|
| | | | hEAAT1 | hEAAT2 | hEAAT3 | rEAAT4 |
| **8a** | 8-Me, 6-Cl |  | >250 [<3.6] | >250 [<3.6] | >250 [<3.6] | >250 [<3.6] |
| **8b** | 8-Me, 6-Cl |  | >250 [<3.6] | >250 [<3.6] | >250 [<3.6] | >250 [<3.6] |
| **8c** | 8-CN |  | >250 [<3.6] | >250 [<3.6] | ~250 [~3.6] | >250 [<3.6] |
| **8d** | 8-CN |  | >250 [<3.6] | >250 [<3.6] | >250 [<3.6] | >250 [<3.6] |
| **8e** | 8-$CF_3$ |  | >250 [<3.6] | >250 [<3.6] | >250 [<3.6] | >250 [<3.6] |
| **8f**[b] | 6-Br | 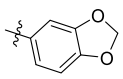 | ~100 [~4.0] | >100 [<4.0] | ~30 [~4.5] | >100 [<4.0] |

[a]Data are based on 3−4 independent experiments ($n$ = 3−4). [b]Obtained from commercial supplier. [c]The inhibitory potencies displayed by the analogues in hEAAT1-HEK293, hEAAT2-HEK293, hEAAT3-HEK293, and rEAAT4-tsA201 cells in the [$^3$H]-D-Asp uptake assay are given.

and m = multiplet), integration value, and coupling constant value in Hz. LC-MS spectra were recorded using a Waters Acquity UPLC-MS instrument with dual wavelength detection with electrospray ionization. Gradients of 5% aqueous MeCN + 0.1% $HCO_2H$ (solvent A) and 95% aqueous MeCN + 0.05% $HCO_2H$ (solvent B) were employed. All compounds tested showed a purity of >95% in HPLC.

*General Procedure A, Three-Component GBB Reaction for the Synthesis of **3a−g, 3i−m, 4b, 4dh, 5d−f, 6c, 7b, 8a−8e, and 10a−10g.*** A 0.5−2 mL Biotage microwave reaction vial was charged with amidine (reactions were performed in scales of 0.3, 0.5, or 1.0 mmol), aldehyde (1.0 equiv), isocyanide (1.0 equiv), and a magnetic stirring bar, purged with nitrogen gas, and sealed with a rubber stopper. The reaction mixture was heated at 160 °C for 1−3 h, monitored by TLC judging by the consumption of the isocyanide substrate. The cooled reaction mixture was dissolved in $CH_2Cl_2$ or EtOAc and co-evaporated with silica gel to give solid residues that were purified by flash column chromatography eluting with heptane and ethyl acetate (or heptane and isopropanol). 2-Methylphenylisocyanide was synthesized in-house using reported procedure,[53] all other isocyanides used in this study were purchased from commercial suppliers. The chemical structures of


DOI: 10.1021/acschemneuro.9b00447
ACS Chem. Neurosci. XXXX, XXX, XXX−XXX

**Table 7. SAR Study of the Impact of Chemical Modifications at Three Positions, the Substituent on the Pyridine Moiety, the Furan Moiety, and the 2-Methylphenyl Moiety, of 3a on EAAT1−4 Activity**[c]

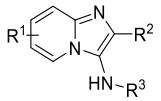


| Cpd. | $R^1$ | $R^2$ | $R^3$ | $IC_{50}$ (μM) [$pIC_{50}$ ± S.E.M.][a] | | | |
|---|---|---|---|---|---|---|---|
| | | | | hEAAT1 | hEAAT2 | hEAAT3 | rEAAT4 |
| **9a**[b] | H | 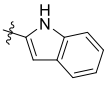 | 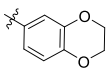 | ~100 [~4.0] | ~100 [~4.0] | ~30 [~4.5] | >100 [<4.0] |
| **9b**[b] | H |  |  | n.t. | n.t. | >250 [<3.6] | n.t. |
| **9c**[b] | H |  |  | n.t. | n.t. | >250 [<3.6] | n.t. |
| **9d**[b] | H |  | 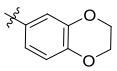 | n.t. | n.t. | >250 [<3.6] | n.t. |
| **9e**[b] | 8-BnO |  |  | n.t. | n.t. | >250 [<3.6] | n.t. |
| **9f**[b] | 8-BnO |  |  | n.t. | n.t. | >250 [<3.6] | n.t. |
| **9g**[b] | 7-Me |  | 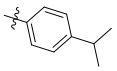 | n.t. | n.t. | >250 [<3.6] | n.t. |
| **9h**[b] | 6-Me |  |  | n.t. | n.t. | ~50 [~4.3] | n.t. |
| **9i**[b] | 6-Me |  |  | n.t. | n.t. | >250 [<3.6] | n.t. |
| **9j**[b] | 6-Me |  | 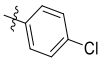 | n.t. | n.t. | >250 [<3.6] | n.t. |
| **9k**[b] | 6-Me |  |  | n.t. | n.t. | >250 [<3.6] | n.t. |
| **9l**[b] | 6-Me |  |  | n.t. | n.t. | >250 [<3.6] | n.t. |
| **9m**[b] | 5-Me |  |  | n.t. | n.t. | ~250 [~3.6] | n.t. |
| **9n**[b] | 5-Me |  |  | n.t. | n.t. | >250 [<3.6] | n.t. |
| **9o**[b] | 5-Me |  |  | n.t. | n.t. | >250 [<3.6] | n.t. |
| **9p**[b] | 5-Me |  |  | n.t. | n.t. | >250 [<3.6] | n.t. |



DOI: 10.1021/acschemneuro.9b00447
ACS Chem. Neurosci. XXXX, XXX, XXX−XXX

**Table 7. continued**

| Cpd. | $R^1$ | $R^2$ | $R^3$ | $IC_{50}$ (μM) [$pIC_{50}$ ± S.E.M.][a] | | | |
|---|---|---|---|---|---|---|---|
| | | | | hEAAT1 | hEAAT2 | hEAAT3 | rEAAT4 |
| **9q**[b] | 6-Br | 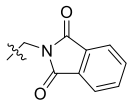 |  | n.t. | n.t. | >250 [<3.6] | n.t. |
| **9r**[b] | 6-Br | 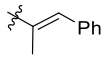 |  | n.t. | n.t. | >250 [<3.6] | n.t. |
| **9s**[b] | 6-Br |  |  | n.t. | n.t. | >250 [<3.6] | n.t. |
| **9t**[b] | 6-Br |  |  | n.t. | n.t. | >250 [<3.6] | n.t. |
| **9u**[b] | 6-Cl | 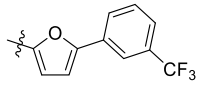 | 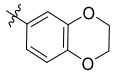 | n.t. | n.t. | >250 [<3.6] | n.t. |
| **9v**[b] | 6-Cl | 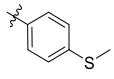 |  | n.t. | n.t. | >250 [<3.6] | n.t. |
| **9w**[b] | 6-Cl |  | 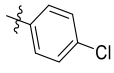 | n.t. | n.t. | >250 [<3.6] | n.t. |
| **9x**[b] | 6-Cl |  |  | n.t. | n.t. | >250 [<3.6] | n.t. |
| **9y**[b] | 6-Cl |  | 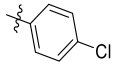 | n.t. | n.t. | >250 [<3.6] | n.t. |
| **9z**[b] | 6-Cl |  | 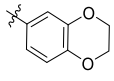 | n.t. | n.t. | >250 [<3.6] | n.t. |
| **9aa**[b] | 6-Cl |  | 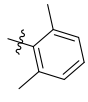 | n.t. | n.t. | >250 [<3.6] | n.t. |
| **9ab**[b] | 5,7-$(Me)_2$ |  | 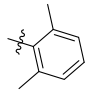 | n.t. | n.t. | ~50 [~4.3] | n.t. |
| **9ac**[b] | 6,8-$(Br)_2$ |  | 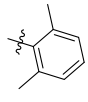 | n.t. | n.t. | >250 [<3.6] | n.t. |

[a]Data are based on 3−4 independent experiments ($n$ = 3−4). [b]Obtained from commercial supplier. n.t., not tested. [c]The inhibitory potencies displayed by the analogues in hEAAT1-HEK293, hEAAT2-HEK293, hEAAT3-HEK293, and rEAAT4-tsA201 cells in the [$^3$H]-D-Asp uptake assay are given.

all final compounds synthesized were confirmed by $^1$H NMR and LC-MS (see the Supporting Information). For compounds of key importance to the SAR study, $^{13}$C NMR was also obtained and is reported below.

*General Procedure B, Microwave-Assisted Suzuki Coupling Reaction for the Synthesis of **3n−z**.* The Suzuki reactions were performed in a Biotage single-mode microwave reactor with a power of 0 to 400 W. A 0.5−2 mL Biotage microwave reaction vial was charged with the bromide substrates **3e−g** (0.5 mmol), boronic acid (1.2 equiv), potassium carbonate (2.0 equiv), XPhos Palladium third generation catalyst (5% mol), and a mixture solvent of THF-$H_2O$ (v/v, 2/1). The vial was sealed with a septum cap, degassed under vacuum, and refilled with a nitrogen atmosphere. After repeating the degassing step three times, the resulting reaction mixture was microwave irradiated for 45 min at 100 °C. The reaction mixture was then cooled to room temperature and filtered through a short pad of Celite. The filtrate was evaporated under vacuum to give the crude substrate, which was purified by flash column chromatography on silica gel eluting with heptane and ethyl acetate.

*2-(Furan-2-yl)-8-methyl-N-(o-tolyl)imidazo[1,2-a]pyridin-3-amine (**3a**).* Prepared from commercially available 2-amino-3-methylpyridine (**11a**, 30 μL, 0.3 mmol), furfural (**12a**, 25 μL, 0.3 mmol), and freshly synthesized 2-methylphenyl isocyanide (**13a**, 37 μL, 0.3 mmol) according to General Procedure A. Purification by flash



DOI: 10.1021/acschemneuro.9b00447
ACS Chem. Neurosci. XXXX, XXX, XXX−XXX

**Table 8. SAR Study of the Impact of Replacement of the Imidazo[1,2-*a*]pyridine Core in 3a with Other Heterocyclic Scaffolds on EAAT1−4 Activity**[b]

Scaffold core

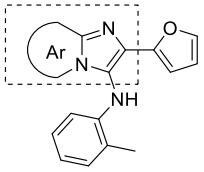


| Cpd. | Scaffold core | IC$_{50}$ (μM) [pIC$_{50}$ ± S.E.M.][a] | | | |
|---|---|---|---|---|---|
| | | hEAAT1 | hEAAT2 | hEAAT3 | rEAAT4 |
| **10a** | 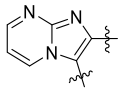 | >250 [<3.6] | >250 [<3.6] | >250 [<3.6] | >250 [<3.6] |
| **10b** | 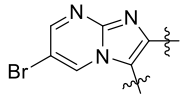 | >250 [<3.6] | >250 [<3.6] | >250 [<3.6] | >250 [<3.6] |
| **10c** | 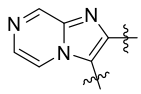 | >250 [<3.6] | >250 [<3.6] | ~250 [~3.6] | >250 [<3.6] |
| **10d** | 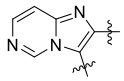 | >250 [<3.6] | >250 [<3.6] | >250 [<3.6] | >250 [<3.6] |
| **10e** | 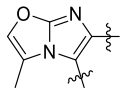 | >250 [<3.6] | >250 [<3.6] | >250 [<3.6] | >250 [<3.6] |
| **10f** | 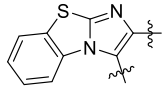 | >250 [<3.6] | >250 [<3.6] | >250 [<3.6] | >250 [<3.6] |
| **10g** | 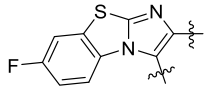 | >250 [<3.6] | >250 [<3.6] | >250 [<3.6] | >250 [<3.6] |

[a]Data are based on 3−4 independent experiments ($n$ = 3−4). [b]The inhibitory potencies displayed by the analogues in hEAAT1-HEK293, hEAAT2-HEK293, hEAAT3-HEK293, and rEAAT4-tsA201 cells in the [$^3$H]-D-Asp uptake assay are given.

column chromatography eluting with heptane and ethyl acetate (v/v, 5/3) gave the target compound **3a** as a yellow solid (41 mg, 45%). $R_f$ = 0.26 (silica gel, heptane/ethyl acetate, 5/3); $R_f$ = 0.22 (silica gel, heptane/iPrOH, 93/7). $^1$H NMR (400 MHz, $CDCl_3$) $\delta$ 7.67 (d, $J$ = 6.8 Hz, 1H), 7.47 (dd, $J$ = 1.8, 0.8 Hz, 1H), 7.20 (d, $J$ = 7.3 Hz, 1H), 7.02 (d, $J$ = 6.8 Hz, 1H), 6.95 (td, $J$ = 7.7, 1.6 Hz, 1H), 6.80 (td, $J$ = 7.4, 1.2 Hz, 1H), 6.76−6.66 (m, 2H), 6.43 (dd, $J$ = 3.4, 1.8 Hz, 1H), 6.09 (dd, $J$ = 8.0, 1.2 Hz, 1H), 5.59 (s, 1H), 2.70 (s, 3H), 2.45 (s, 3H). $^{13}$C NMR (100 MHz, $CDCl_3$): $\delta$ 148.7, 143.2, 142.5, 142.3, 130.9, 130.8, 127.7, 127.4, 124.0, 122.8, 120.6, 119.9, 118.8, 112.5, 112.2, 111.4, 107.6, 17.6, 16.8. MS (ESI+) $m/z$: 304.1 [M + H]$^+$.

*2-(Furan-2-yl)-7-methyl-N-(o-tolyl)imidazo[1,2-a]pyridin-3-amine (**3b**).* Prepared from commercially available 2-amino-4-methylpyridine (35 μL, 0.35 mmol), furfural (**12a**, 29 μL, 0.35 mmol), and freshly synthesized 2-methylphenyl isocyanide (**13a**, 43 μL, 0.35 mmol) according to General Procedure A. Purification by flash column chromatography eluting with heptane and ethyl acetate (v/v, 3/2) gave the target compound **3b** as a yellow solid (65 mg, 61%). $R_f$ = 0.31 (silica gel, heptane/ethyl acetate, 1/1); $R_f$ = 0.26 (silica gel, heptane/iPrOH, 9/1). $^1$H NMR (400 MHz, $CDCl_3$) $\delta$ 7.64 (d, $J$ = 6.9 Hz, 1H), 7.43 (s, 1H), 7.36 (s, 1H), 7.19 (d, $J$ = 7.4 Hz, 1H), 6.94 (t, $J$ = 7.7 Hz, 1H), 6.79 (t, $J$ = 7.4 Hz, 1H), 6.67 (s, 1H), 6.58 (d, $J$ = 7.0 Hz, 1H), 6.42 (s, 1H), 6.08 (d, $J$ = 8.1 Hz, 1H), 5.61 (s, 1H), 2.44 (s, 3H), 2.39 (s, 3H). $^{13}$C NMR (101 MHz, $CDCl_3$) $\delta$ 149.0, 143.3, 142.7, 142.1, 136.1, 130.8, 130.7, 127.4, 122.8, 122.0, 119.8, 118.1, 116.0, 114.9, 112.2, 111.4, 107.3, 21.4, 17.6. MS (ESI+) $m/z$: 304.1 [M + H]$^+$.

*8-Bromo-2-(furan-2-yl)-N-(o-tolyl)imidazo[1,2-a]pyridin-3-amine (**3e**).* Prepared from commercially available 2-amino-3-bromopyridine (86 mg, 0.5 mmol), furfural (**12a**, 42 μL, 0.5 mmol), and freshly synthesized 2-methylphenyl isocyanide (**13a**, 62 μL, 0.5 mmol) according to General Procedure A. Purification by flash column chromatography eluting with heptane and ethyl acetate (v/v, 5/1) gave the target compound **3e** as a yellow solid (96 mg, 52%). $R_f$ = 0.36 (silica gel, heptane/ethyl acetate, 3/1). $^1$H NMR (600 MHz, $CDCl_3$) $\delta$ 7.76 (dd, $J$ = 6.7, 1.0 Hz, 1H), 7.48 (dd, $J$ = 7.2, 1.0 Hz, 1H), 7.46 (d, $J$ = 1.8 Hz, 1H), 7.21 (d, $J$ = 7.4 Hz, 1H), 6.96 (t, $J$ = 8.1 Hz, 1H), 6.82 (t, $J$ = 7.4 Hz, 1H), 6.79 (d, $J$ = 3.5 Hz, 1H), 6.66 (t, $J$ = 7.0 Hz, 1H), 6.44 (dd, $J$ = 3.4, 1.8 Hz, 1H), 6.06 (dd, $J$ = 8.0, 1.2 Hz, 1H), 5.69 (s, 1H), 2.46 (s,


DOI: 10.1021/acschemneuro.9b00447
ACS Chem. Neurosci. XXXX, XXX, XXX−XXX

3H). $^{13}$C NMR (151 MHz, $CDCl_3$) $\delta$ 148.3, 142.6, 142.1, 140.5, 131.9, 130.9, 127.43, 127.36, 123.2, 122.3, 120.3, 120.1, 112.36, 112.35, 111.7, 111.5, 108.5, 17.7. MS (ESI+) $m/z$: 368.1 [M + H, $^{79}$Br]$^+$, 370.1 [M + H, $^{81}$Br]$^+$.

*7-Bromo-2-(furan-2-yl)-N-(o-tolyl)imidazo[1,2-a]pyridin-3-amine (**3f**).* Prepared from commercially available 2-amino-4-bromopyridine (86 mg, 0.5 mmol), furfural (**12a**, 42 $\mu$L, 0.5 mmol), and freshly synthesized 2-methylphenyl isocyanide (**13a**, 62 $\mu$L, 0.5 mmol) according to General Procedure A. Purification by flash column chromatography eluting with heptane and ethyl acetate (v/v, 4/1) gave the target compound **3f** as a yellow solid (102 mg, 56%). $R_f$ = 0.33 (silica gel, heptane/ethyl acetate, 3/1). $^1$H NMR (600 MHz, $CDCl_3$) $\delta$ 7.80 (dd, $J$ = 1.8, 0.8 Hz, 1H), 7.63 (dd, $J$ = 7.2, 0.8 Hz, 1H), 7.45 (dd, $J$ = 1.8, 0.8 Hz, 1H), 7.21 (d, $J$ = 7.4 Hz, 2H), 6.99−6.93 (m, 1H), 6.88 (dd, $J$ = 7.2, 1.9 Hz, 1H), 6.82 (td, $J$ = 7.4, 1.2 Hz, 1H), 6.73 (dd, $J$ = 3.4, 0.8 Hz, 1H), 6.45 (dd, $J$ = 3.4, 1.8 Hz, 1H), 6.05 (d, $J$ = 8.0 Hz, 1H), 5.66 (s, 1H), 2.45 (s, 3H). $^{13}$C NMR (151 MHz, $CDCl_3$) $\delta$ 148.3, 142.7, 142.7, 142.1, 131.4, 131.0, 127.5, 123.2, 123.2, 120.4, 119.7, 119.1, 119.0, 116.4, 112.3, 111.6, 108.2, 17.7. MS (ESI+) $m/z$: 368.1 [M + H, $^{79}$Br]$^+$, 370.1 [M + H, $^{81}$Br]$^+$.

*8-Bromo-2-(furan-2-yl)-7-methyl-N-(o-tolyl)imidazo[1,2-a]pyridin-3-amine (**3m**).* Prepared from commercially available 2-amino-3-bromo-4-methylpyridine (94 mg, 0.5 mmol), furfural (**12a**, 42 $\mu$L, 0.5 mmol), and freshly synthesized 2-methylphenyl isocyanide (**13a**, 62 $\mu$L, 0.5 mmol) according to General Procedure A. Purification by flash column chromatography eluting with heptane and ethyl acetate (v/v, 3/1) gave the target compound **3m** as a yellow solid (102 mg, 56%). $R_f$ = 0.33 (silica gel, heptane/ethyl acetate, 3/1). $^1$H NMR (600 MHz, $CDCl_3$) $\delta$ 7.63 (d, $J$ = 6.8 Hz, 1H), 7.44 (dd, $J$ = 1.8, 0.8 Hz, 1H), 7.20 (d, $J$ = 7.5 Hz, 1H), 6.97−6.91 (m, 1H), 6.81 (td, $J$ = 7.4, 1.2 Hz, 1H), 6.74 (d, $J$ = 3.4 Hz, 1H), 6.63 (d, $J$ = 6.8 Hz, 1H), 6.42 (dd, $J$ = 3.4, 1.8 Hz, 1H), 6.07 (d, $J$ = 8.1 Hz, 1H), 5.64 (s, 1H), 2.50 (s, 3H), 2.45 (s, 3H). $^{13}$C NMR (151 MHz, $CDCl_3$) $\delta$ 148.5, 142.4, 142.4, 141.2, 135.2, 131.7, 130.9, 127.4, 123.0, 121.0, 120.1, 119.6, 115.0, 112.3, 112.2, 111.4, 108.1, 22.1, 17.6. MS (ESI+) $m/z$: 382.0 [M + H, $^{79}$Br]$^+$, 384.1 [M + H, $^{81}$Br]$^+$.

*tert-Butyl 3-(8-methyl-3-(o-tolylamino)imidazo[1,2-a]pyridin-2-yl)azetidine-1-carboxylate (**4g**).* Prepared from commercially available 2-amino-3-methylpyridine (**11a**, 50 $\mu$L, 0.5 mmol), *N*-Boc-azetidine-3-carbaldehyde (**12b**, 93 mg, 0.5 mmol) and freshly synthesized 2-methylphenyl isocyanide (**13a**, 62 $\mu$L, 0.5 mmol) according to General Procedure A. Purification by flash column chromatography eluting with heptane and ethyl acetate (v/v, 1/2) gave the target compound **4g** as a light yellow solid (132 mg, 67%). $R_f$ = 0.27 (silica gel, heptane/ethyl acetate, 2/5). $^1$H NMR (400 MHz, $CDCl_3$) $\delta$ 7.71 (d, $J$ = 6.8 Hz, 1H), 7.22−7.13 (m, 1H), 7.08−7.02 (m, 1H), 6.99−6.90 (m, 1H), 6.83−6.70 (m, 2H), 6.00 (dd, $J$ = 8.1, 1.2 Hz, 1H), 5.30 (s, 1H), 4.23 (dd, $J$ = 7.6, 1.9 Hz, 4H), 3.99 (s, 1H), 2.67 (s, 3H), 2.38 (s, 3H), 1.41 (s, 9H). $^{13}$C NMR (151 MHz, $CDCl_3$) $\delta$ 156.4, 142.5, 141.4, 138.9, 131.1, 127.5, 126.8, 122.5, 120.7, 120.1, 119.6, 113.5, 111.5, 79.6, 54.5, 28.4, 26.4, 17.6, 16.9. MS (ESI+) $m/z$: 293.0 [M + H, -Boc]$^+$.

*1-(3-(8-Methyl-3-(o-tolylamino)imidazo[1,2-a]pyridin-2-yl)-azetidin-1-yl)ethan-1-one (**4h**) and N-(3-Chloro-2-(8-methyl-3-(o-tolylamino)imidazo[1,2-a]pyridin-2-yl)propyl)acetamide (**4i**).* *tert*-Butyl 3-(8-methyl-3-(*o*-tolylamino)imidazo[1,2-*a*]pyridin-2-yl)-azetidine-1-carboxylate (**4g**, 24 mg, 0.06 mmol) was dissolved in HCl solution (4.0 M in dioxane, 0.6 mL). After stirring the reaction mixture at room temperature for 30 min, the solvent was evaporated under vacuum to give a solid residue, which was suspended in $CH_2Cl_2$ (0.6 mL), and $Et_3N$ (22 $\mu$L, 0.16 mmol) and acetyl chloride (4.3 $\mu$L, 0.06 mmol) were added. The resulting mixture was stirred at room temperature for 1 h before evaporation under vacuum to give an oil residue. Purification by flash column chromatography eluting with heptane and iPrOH (v/v, 9/1) gave the target compound **4i** as a white solid (7 mg, 31%), and switching the eluting system to heptane and iPrOH (v/v, 3/2) gave the target compound **4h** as a white solid (8 mg, 40%). For **4h**: $^1$H NMR (600 MHz, $CDCl_3$) $\delta$ 7.70 (d, $J$ = 6.7 Hz, 1H), 7.17 (d, $J$ = 7.8 Hz, 1H), 7.10 (d, $J$ = 6.9 Hz, 1H), 6.95 (t, $J$ = 7.6 Hz, 1H), 6.83−6.74 (m, 2H), 6.00 (d, $J$ = 8.1 Hz, 1H), 5.40 (s, 1H), 4.48 (dd, $J$ = 8.2, 6.2 Hz, 1H), 4.41 (t, $J$ = 8.6 Hz, 1H), 4.33−4.27 (m, 2H), 4.10−4.02 (m, 1H), 2.68 (s, 3H), 2.39 (s, 3H), 1.77 (s, 3H). $^{13}$C NMR (151 MHz, $CDCl_3$) $\delta$ 170.8, 142.8, 142.1, 139.5, 131.1, 127.4, 127.1, 125.2, 122.3, 120.6, 120.0, 119.4, 113.1, 111.4, 55.7, 53.4, 26.1, 18.7, 17.6, 16.8. MS (ESI+) $m/z$: 335.2 [M + H]$^+$.

For **4i**: $^1$H NMR (400 MHz, $CDCl_3$) $\delta$ 7.67 (d, $J$ = 6.8 Hz, 1H), 7.23−7.04 (m, 3H), 6.94 (t, $J$ = 7.4 Hz, 1H), 6.87−6.70 (m, 2H), 6.13−5.93 (m, 2H), 4.01 (ddd, $J$ = 14.6, 8.6, 7.3 Hz, 1H), 3.84 (qd, $J$ = 11.0, 6.9 Hz, 2H), 3.57 (dq, $J$ = 8.4, 4.4 Hz, 2H), 2.66 (s, 3H), 2.43 (s, 3H), 1.89 (s, 3H). $^{13}$C NMR (101 MHz, $CDCl_3$) $\delta$ 170.9, 142.7, 141.9, 137.3, 131.1, 127.3, 126.7, 125.4, 122.7, 121.2, 121.1, 119.8, 113.1, 111.4, 46.1, 41.1, 40.4, 23.3, 17.6, 16.7. MS (ESI+) $m/z$: 371.2 [M + H]$^+$.

*(2-Fluorophenyl)(3-(8-methyl-3-(o-tolylamino)imidazo[1,2-a]-pyridin-2-yl)azetidin-1-yl)methanone (**4j**) and N-(3-Chloro-2-(8-methyl-3-(o-tolylamino)imidazo[1,2-a]pyridin-2-yl)propyl)-2-fluorobenzamide (**4k**).* Prepared from *tert*-butyl 3-(8-methyl-3-(o-tolylamino)imidazo[1,2-*a*]pyridin-2-yl)azetidine-1-carboxylate (**4g**, 24 mg, 0.06 mmol) and 2-fluorobenzoyl chloride (7.2 $\mu$L, 0.06 mmol) according to the procedure described for the synthesis of compounds **4h** and **4i**. Purification by flash column chromatography eluting with heptane and ethyl acetate (v/v, 7/3) gave the target compound **4k** as a yellow solid (8 mg, 29%), and switching the eluting system to heptane and ethyl acetate (v/v, 1/9) gave the target compound **4j** as a yellow solid (12 mg, 48%). For **4j**: $^1$H NMR (600 MHz, $CDCl_3$) $\delta$ 7.67 (d, $J$ = 6.8 Hz, 1H), 7.45 (td, $J$ = 7.3, 1.8 Hz, 1H), 7.41−7.34 (m, 1H), 7.19−7.12 (m, 2H), 7.10−7.02 (m, 2H), 6.93 (t, $J$ = 7.6 Hz, 1H), 6.78 (t, $J$ = 7.4 Hz, 1H), 6.75 (s, 1H), 5.99 (d, $J$ = 8.1 Hz, 1H), 5.32 (s, 1H), 4.51 (d, $J$ = 7.8 Hz, 2H), 4.49−4.44 (m, 1H), 4.38 (t, $J$ = 8.8 Hz, 1H), 4.15 (s, 1H), 2.67 (s, 3H), 2.39 (s, 3H). $^{13}$C NMR (151 MHz, $CDCl_3$) $\delta$ 166.5, 159.0 (d, $^1J_{CF}$ = 250.3 Hz), 142.7, 142.0, 139.2, 132.1 (d, $^3J_{CF}$ = 8.2 Hz), 131.1, 130.1 (d, $^4J_{CF}$ = 3.4 Hz), 127.5, 127.3, 125.1, 124.5 (d, $^3J_{CF}$ = 3.4 Hz), 122.3, 122.2 (d, $^2J_{CF}$ = 16.4 Hz), 120.6, 120.0, 119.3, 116.0 (d, $^2J_{CF}$ = 22.1 Hz), 112.9, 111.4, 56.4, 53.8, 27.0, 17.5, 16.8. MS (ESI+) $m/z$: 415.2 [M + H]$^+$.

For **4k**: $^1$H NMR (400 MHz, $CDCl_3$) $\delta$ 8.11 (s, 1H), 7.98 (td, $J$ = 7.8, 1.9 Hz, 1H), 7.67 (d, $J$ = 6.8 Hz, 1H), 7.49−7.37 (m, 1H), 7.21 (td, $J$ = 7.6, 1.1 Hz, 1H), 7.19−7.11 (m, 2H), 7.08 (ddd, $J$ = 11.9, 8.3, 1.1 Hz, 1H), 6.91−6.72 (m, 3H), 6.00 (d, $J$ = 8.0 Hz, 1H), 5.89 (s, 1H), 4.35−4.23 (m, 1H), 4.07−3.90 (m, 2H), 3.83 (dt, $J$ = 13.4, 4.4 Hz, 1H), 3.77 (s, 1H), 2.71 (s, 3H), 2.42 (s, 3H). $^{13}$C NMR (101 MHz, $CDCl_3$) $\delta$ 164.1, 160.6 (d, $^1J_{CF}$ = 249.1 Hz), 142.4, 141.7, 136.9, 133.2 (d, $^3J_{CF}$ = 9.2 Hz), 131.8 (d, $^4J_{CF}$ = 1.9 Hz), 131.0, 127.4, 126.9, 126.2, 124.6 (d, $^3J_{CF}$ = 3.4 Hz), 122.8, 121.5 (d, $^2J_{CF}$ = 13.7 Hz), 121.4, 121.1, 120.0, 116.1 (d, $^2J_{CF}$ = 24.2 Hz), 113.5, 111.7, 46.0, 41.8, 39.7, 17.5, 16.7. MS (ESI+) $m/z$: 451.2 [M + H]$^+$.

*tert-Butyl 3-(8-bromo-7-methyl-3-(o-tolylamino)imidazo[1,2-a]-pyridin-2-yl)azetidine-1-carboxylate (**7b**).* Prepared from commercially available 2-amino-3-bromo-4-methylpyridine (**12m**, 94 mg, 0.5 mmol), *N*-Boc-azetidine-3-carbaldehyde (**12b**, 93 mg, 0.5 mmol), and freshly synthesized 2-methylphenyl isocyanide (**13a**, 62 $\mu$L, 0.5 mmol) according to General Procedure A. Purification by flash column chromatography eluting with heptane and ethyl acetate (v/v, 1/3) gave the target compound **7b** as an off-white solid (119 mg, 51%). $R_f$ = 0.31 (silica gel, heptane/ethyl acetate, 2/5). $^1$H NMR (600 MHz, $CDCl_3$) $\delta$ 7.63 (d, $J$ = 6.8 Hz, 1H), 7.16 (d, $J$ = 7.4 Hz, 1H), 6.94 (t, $J$ = 8.0 Hz, 1H), 6.78 (t, $J$ = 7.4 Hz, 1H), 6.64 (d, $J$ = 6.8 Hz, 1H), 5.98 (d, $J$ = 8.0 Hz, 1H), 5.33 (s, 1H), 4.26−4.17 (m, 4H), 3.99−3.91 (m, 1H), 2.50 (s, 3H), 2.37 (s, 3H), 1.40 (s, 9H). $^{13}$C NMR (151 MHz, $CDCl_3$) $\delta$ 156.4, 142.8, 142.0, 140.8, 135.0, 131.0, 127.5, 122.2, 120.7, 119.9, 114.9, 112.2, 111.5, 79.3, 54.5, 28.4, 27.3, 22.0, 17.5. MS (ESI+) $m/z$: 471.2 [M + H, $^{79}$Br]$^+$, 473.1 [M + H, $^{81}$Br]$^+$.

**Pharmacology.** *Materials.* Culture media, serum, antibiotics and buffers for cell culture and assays were obtained from Invitrogen (Paisley, UK). The FLIPR Membrane Potential Blue assay dye was purchased from Molecular Devices (Crawley, UK), and [$^3$H]-D-Asp was obtained from PerkinElmer (Boston, MA). (*S*)-Glu was purchased from Sigma (St. Louis, MO). If not otherwise stated, all chemicals for the screening were purchased from Sigma (St. Louis, MO). The compound libraries included in the screening (ChemDiv6, Biomol 4,


DOI: 10.1021/acschemneuro.9b00447
ACS Chem. Neurosci. XXXX, XXX, XXX−XXX

Microsource 1, Prestwick2, LOPAC 1, Chembridge GPCR, Chembridge Ion Channel, Chembridge Kinase Core, and eMolecules) were obtained from ICCB-Longwood, Harvard Medical School (Boston, MA). The stable hEAAT1-, hEAAT2-, and hEAAT3-HEK293 cell lines have been described previously,[39] and the stable rEAAT4-tsA201 cell line was a generous gift from Drs. Peter Kovermann and Christoph Fahlke and has been characterized pharmacologically in a previous study.[47]

*Cell Culture.* All cell lines were cultured at 37 °C in a humidified 5% $CO_2$ atmosphere. The hEAAT1-, hEAAT2-, and hEAAT3-HEK293 cell lines were maintained in Culture Medium I [Dulbecco's modified Eagle's medium Glutamax-I (DMEM) supplemented with 5% dialyzed fetal bovine serum, 100 U/mL penicillin, 100 μg/mL streptomycin ,and 1 mg/mL G-418], and the stable rEAAT4-tsA201 cell line was maintained in Culture Medium II [DMEM supplemented with 5% tetracycline-free fetal bovine serum, 100 U/mL penicillin, 100 μg/mL streptomycin, 0.2 mg/mL hygromycin B, and 10 μg/mL blasticidin].

*Compound Library Screening at hEAAT3.* The compound library screening was performed at ICCB-Longwood, Harvard Medical School (Boston, MA). hEAAT3-HEK293 cells ($10^5$ cells/well) were seeded in 20 μL of Culture Medium I into Corning CellBIND 384 well plates (Corning, New York, NY) using a WellMate Multidrop (Thermofisher Scientific, Waltham, MA) and incubated in the cell incubator overnight. The following day, cells were gently washed in 40 μL of KREBS buffer (140 mM NaCl, 4.7 mM KCl, 2.5 mM $CaCl_2$, 1.2 mM $MgCl_2$, 11 mM HEPES, 10 mM D-glucose, pH 7.4) using a WellMate Multidrop, then 30 μL of 0.5 g/mL FMP Blue in KREBS buffer was added using a BRAVO apparatus (Agilent, Santa Clara, CA), and the plates were incubated for 1 h in the cell culture incubator. Compounds were prepared by adding 300 nL of the stock (10 mM or 2 g/L in DMSO, depending on library) to 30 μL of KREBS buffer with 1.2 mM Glu in 384-well polypropylene plates (Greiner Bio-One, Kremsmünster, Austria) using a Seiko Compound Transfer Robot SGM 611 (Seiko, Tokyo, Japan). KREBS buffer with either 0.1% DMSO or 1.2 mM Glu and 0.1% DMSO was prepared for controls. Assay plates and compound plates were transferred to a Hamamatsu FDSS7000EX plate reader (Hamamatsu Photonics K.K., Shizuoka, Japan) equipped with a Semrock FF02-531/22 excitation filter and FF01-593/46 emission filter (Semrock, Rochester, NY) and a Hamamatsu DM565 nm dichroic mirror. Exposure time was set to 200 ms, and sensitivity was set manually on a "per plate" basis (typically set to 2). Cells were measured for 134 s, and compounds were triturated thrice immediately prior to addition. Then 10 μL of compounds was transferred at 10 μL/s after 20 s of measurement. Sampling occurred every 1 s for 18 s, then every 500 ms for 65 s, and every 1 s for the remaining time. Compounds were screened twice at the transporter, in different plates on the same day.

*[$^3$H]-D-Asp Uptake Assay.* The pharmacological characterization of various reference EAAT ligands and test compounds in the [$^3$H]-D-Asp uptake assay was performed essentially as described previously.[47] The day before the assay cells were split into poly-D-lysine-coated white 96-well plates (PerkinElmer, Boston, MA) in Culture Medium I (hEAAT1-, hEAAT2-, and hEAAT3-HEK293) or in Culture Medium II supplemented with 1 μg/mL tetracycline (rEAAT4-tsA201). At 16–24 h later, the culture medium was aspirated and cells were washed twice with 100 μL of assay buffer (Hank's buffered saline solution supplemented with 20 mM HEPES, 1 mM $CaCl_2$ and 1 mM $MgCl_2$, pH 7.4). Then 50 μL of assay buffer supplemented with 100 nM [$^3$H]-D-Asp (PerkinElmer, Boston, MA) and various concentrations of test compounds were added to the wells, and the plate was incubated at 37 °C for 4 min. Nonspecific [$^3$H]-D-Asp uptake/binding in the cells was determined in the presence of 3 mM Glu. The assay mixtures were quickly removed from the wells, and the wells were washed with 2 × 100 μL ice-cold assay buffer, after which 150 μL Microscint[20] scintillation fluid (PerkinElmer, Boston, MA) was added to each well. Then the plate was shaken for at least 1h and counted in a TopCounter (PerkinElmer, Boston, MA). The experiments were performed in duplicate 3–4 times for each compound.

*Data Analysis.* Data from the screening in the FDSS was analyzed using Screensaver (ICCB-Longwood, Boston, MA) and Vortex (CM Laboratories Simulations) to yield end point changes in fluorescence ratios. Subsequent analysis was done using MS Excels 2016 and GraphPad Prism 7. Compounds that inhibited the Glu-induced change in fluorescence by at least 50%, compared to buffer with vehicle, in both duplicates, were considered hits.

The data obtained in the [$^3$H]-D-Asp uptake assay were fitted to the equation % uptake = 100% uptake/$[1 + ([L]/IC_{50})^{nH}]$, and $IC_{50}$ values for the test compounds were derived from this equation. Concentration–inhibition curves were generated by nonweighted least-squares fits using GraphPad Prism 8.0.

## ■ ASSOCIATED CONTENT

### Supporting Information

The Supporting Information is available free of charge on the ACS Publications website at DOI: 10.1021/acschemneuro.9b00447.

$^1$H NMR and LCMS data for compounds **3b**,**d**,**g**,**i**–**n**,**o**–**z**, **4b**,**d**–**f**, **5d**–**f**, **6c**, **8a**–**d**, and **10a**–**g** (PDF)

## ■ AUTHOR INFORMATION


### Corresponding Authors

*E-mail: aaj@sund.ku.dk (A.A.J., pharmacology).
*E-mail: lebu@sund.ku.dk (L.B., chemistry).

### ORCID

Peng Wu: 0000-0002-0186-1086
Lennart Bunch: 0000-0002-0180-4639


### Author Contributions

P.W. and W.E.B.-Y. contributed equally to this work and are co-first authors. P.W.: Medicinal chemistry, manuscript preparation. W.E.B.-Y.: Pharmacology, manuscript preparation. M.S.: Medicinal chemistry, manuscript preparation. A.A.J.: Pharmacology, medicinal chemistry, manuscript preparation. L.B.: Medicinal chemistry, manuscript preparation.


### Funding

The authors thank the Danish Council of Independent Research for Medical Sciences and the Lundbeck Foundation (R209-2015-3204) for financial support.


### Notes

The authors declare no competing financial interest.

## ■ ACKNOWLEDGMENTS


Drs. Peter Kovermann and Christoph Fahlke are thanked for their generous gift of the stable rEAAT4-tsA201 cell line. Drs. Lee Barrett and Alyssa Grant from the Woolf Lab and Drs. Jennifer Smith and Rachel Warden from the ICCB-Longwood, Harvard Medical School are thanked for their assistance with the screen and with the compound libraries, respectively.


## ■ REFERENCES


(1) Danbolt, N. C. (2001) Glutamate uptake. *Prog. Neurobiol. 65*, 1–105.

(2) Jensen, A. A., Fahlke, C., Bjørn-Yoshimoto, W. E., and Bunch, L. (2015) Excitatory amino acid transporters: recent insights into molecular mechanisms, novel modes of modulation and new therapeutic possibilities. *Curr. Opin. Pharmacol. 20*, 116–123.

(3) Grewer, C., Gameiro, A., and Rauen, T. (2014) SLC1 glutamate transporters. *Pfluegers Arch. 466*, 3–24.

(4) Bunch, L., Erichsen, M. N., and Jensen, A. A. (2009) Excitatory amino acid transporters as potential drug targets. *Expert Opin. Ther. Targets 13*, 719–31.

(5) Jiang, J., and Amara, S. G. (2011) New views of glutamate transporter structure and function: advances and challenges. *Neuropharmacology 60*, 172–81.




DOI: 10.1021/acschemneuro.9b00447
*ACS Chem. Neurosci.* XXXX, XXX, XXX–XXX

(6) Vandenberg, R. J., and Ryan, R. M. (2013) Mechanisms of glutamate transport. *Physiol. Rev. 93*, 1621−57.
(7) Rose, C. R., Ziemens, D., Untiet, V., and Fahlke, C. (2018) Molecular and cellular physiology of sodium-dependent glutamate transporters. *Brain Res. Bull. 136*, 3−16.
(8) Sheldon, A. L., and Robinson, M. B. (2007) The role of glutamate transporters in neurodegenerative diseases and potential opportunities for intervention. *Neurochem. Int. 51*, 333−55.
(9) Sattler, R., and Rothstein, J. D. (2006) Regulation and dysregulation of glutamate transporters. *Handb Exp Pharmacol 175*, 277−303.
(10) Gegelashvili, G., and Bjerrum, O. J. (2014) High-affinity glutamate transporters in chronic pain: an emerging therapeutic target. *J. Neurochem. 131*, 712−30.
(11) Rothstein, J. D., Patel, S., Regan, M. R., Haenggeli, C., Huang, Y. H., Bergles, D. E., Jin, L., Dykes Hoberg, M., Vidensky, S., Chung, D. S., Toan, S. V., Bruijn, L. I., Su, Z. Z., Gupta, P., and Fisher, P. B. (2005) Beta-lactam antibiotics offer neuroprotection by increasing glutamate transporter expression. *Nature 433*, 73−7.
(12) Bjørn-Yoshimoto, W. E., and Underhill, S. M. (2016) The importance of the excitatory amino acid transporter 3 (EAAT3). *Neurochem. Int. 98*, 4−18.
(13) Scimemi, A., Tian, H., and Diamond, J. S. (2009) Neuronal transporters regulate glutamate clearance, NMDA receptor activation, and synaptic plasticity in the hippocampus. *J. Neurosci. 29*, 14581−95.
(14) Jarzylo, L. A., and Man, H. Y. (2012) Parasynaptic NMDA receptor signaling couples neuronal glutamate transporter function to AMPA receptor synaptic distribution and stability. *J. Neurosci. 32*, 2552−63.
(15) Underhill, S. M., Wheeler, D. S., Li, M., Watts, S. D., Ingram, S. L., and Amara, S. G. (2014) Amphetamine modulates excitatory neurotransmission through endocytosis of the glutamate transporter EAAT3 in dopamine neurons. *Neuron 83*, 404−416.
(16) Underhill, S. M., Ingram, S. L., Ahmari, S. E., Veenstra-VanderWeele, J., and Amara, S. G. (2019) Neuronal excitatory amino acid transporter EAAT3: Emerging functions in health and disease. *Neurochem. Int. 123*, 69−76.
(17) Sepkuty, J. P., Cohen, A. S., Eccles, C., Rafiq, A., Behar, K., Ganel, R., Coulter, D. A., and Rothstein, J. D. (2002) A neuronal glutamate transporter contributes to neurotransmitter GABA synthesis and epilepsy. *J. Neurosci. 22*, 6372−9.
(18) Mathews, G. C., and Diamond, J. S. (2003) Neuronal glutamate uptake contributes to GABA synthesis and inhibitory synaptic strength. *J. Neurosci. 23*, 2040−8.
(19) Dericioglu, N., Garganta, C. L., Petroff, O. A., Mendelsohn, D., and Williamson, A. (2008) Blockade of GABA synthesis only affects neural excitability under activated conditions in rat hippocampal slices. *Neurochem. Int. 53*, 22−32.
(20) Aoyama, K., Suh, S. W., Hamby, A. M., Liu, J., Chan, W. Y., Chen, Y., and Swanson, R. A. (2006) Neuronal glutathione deficiency and age-dependent neurodegeneration in the EAAC1 deficient mouse. *Nat. Neurosci. 9*, 119−26.
(21) Harada, T., Harada, C., Nakamura, K., Quah, H. M., Okumura, A., Namekata, K., Saeki, T., Aihara, M., Yoshida, H., Mitani, A., and Tanaka, K. (2007) The potential role of glutamate transporters in the pathogenesis of normal tension glaucoma. *J. Clin. Invest. 117*, 1763−70.
(22) Won, S. J., Yoo, B. H., Brennan, A. M., Shin, B. S., Kauppinen, T. M., Berman, A. E., Swanson, R. A., and Suh, S. W. (2010) EAAC1 gene deletion alters zinc homeostasis and exacerbates neuronal injury after transient cerebral ischemia. *J. Neurosci. 30*, 15409−18.
(23) Berman, A. E., Chan, W. Y., Brennan, A. M., Reyes, R. C., Adler, B. L., Suh, S. W., Kauppinen, T. M., Edling, Y., and Swanson, R. A. (2011) N-acetylcysteine prevents loss of dopaminergic neurons in the EAAC1−/− mouse. *Ann. Neurol. 69*, 509−20.
(24) Sung, B., Lim, G., and Mao, J. (2003) Altered expression and uptake activity of spinal glutamate transporters after nerve injury contribute to the pathogenesis of neuropathic pain in rats. *J. Neurosci. 23*, 2899−910.
(25) Mao, J., Sung, B., Ji, R. R., and Lim, G. (2002) Neuronal apoptosis associated with morphine tolerance: evidence for an opioid-induced neurotoxic mechanism. *J. Neurosci. 22*, 7650−61.
(26) Guo, M., Cao, D., Zhu, S., Fu, G., Wu, Q., Liang, J., and Cao, M. (2015) Chronic exposure to morphine decreases the expression of EAAT3 via opioid receptors in hippocampal neurons. *Brain Res. 1628*, 40−9.
(27) Nakagawa, T., Ozawa, T., Shige, K., Yamamoto, R., Minami, M., and Satoh, M. (2001) Inhibition of morphine tolerance and dependence by MS-153, a glutamate transporter activator. *Eur. J. Pharmacol. 419*, 39−45.
(28) Bailey, C. G., Ryan, R. M., Thoeng, A. D., Ng, C., King, K., Vanslambrouck, J. M., Auray-Blais, C., Vandenberg, R. J., Broer, S., and Rasko, J. E. (2011) Loss-of-function mutations in the glutamate transporter SLC1A1 cause human dicarboxylic aminoaciduria. *J. Clin. Invest. 121*, 446−53.
(29) Delgado-Acevedo, C., Estay, S. F., Radke, A. K., Sengupta, A., Escobar, A. P., Henriquez-Belmar, F., Reyes, C. A., Haro-Acuna, V., Utreras, E., Sotomayor-Zarate, R., Cho, A., Wendland, J. R., Kulkarni, A. B., Holmes, A., Murphy, D. L., Chavez, A. E., and Moya, P. R. (2019) Behavioral and synaptic alterations relevant to obsessive-compulsive disorder in mice with increased EAAT3 expression. *Neuropsychopharmacology 44*, 1163.
(30) Zike, I. D., Chohan, M. O., Kopelman, J. M., Krasnow, E. N., Flicker, D., Nautiyal, K. M., Bubser, M., Kellendonk, C., Jones, C. K., Stanwood, G., Tanaka, K. F., Moore, H., Ahmari, S. E., and Veenstra-VanderWeele, J. (2017) OCD candidate gene SLC1A1/EAAT3 impacts basal ganglia-mediated activity and stereotypic behavior. *Proc. Natl. Acad. Sci. U. S. A. 114*, 5719−5724.
(31) Samuels, J., Wang, Y., Riddle, M. A., Greenberg, B. D., Fyer, A. J., McCracken, J. T., Rauch, S. L., Murphy, D. L., Grados, M. A., Knowles, J. A., Piacentini, J., Cullen, B., Bienvenu, O. J., 3rd, Rasmussen, S. A., Geller, D., Pauls, D. L., Liang, K. Y., Shugart, Y. Y., and Nestadt, G. (2011) Comprehensive family-based association study of the glutamate transporter gene SLC1A1 in obsessive-compulsive disorder. *Am. J. Med. Genet., Part B 156B*, 472−7.
(32) Stewart, S. E., Mayerfeld, C., Arnold, P. D., Crane, J. R., O'Dushlaine, C., Fagerness, J. A., Yu, D., Scharf, J. M., Chan, E., Kassam, F., Moya, P. R., Wendland, J. R., Delorme, R., Richter, M. A., Kennedy, J. L., Veenstra-VanderWeele, J., Samuels, J., Greenberg, B. D., McCracken, J. T., Knowles, J. A., Fyer, A. J., Rauch, S. L., Riddle, M. A., Grados, M. A., Bienvenu, O. J., Cullen, B., Wang, Y., Shugart, Y. Y., Piacentini, J., Rasmussen, S., Nestadt, G., Murphy, D. L., Jenike, M. A., Cook, E. H., Pauls, D. L., Hanna, G. L., and Mathews, C. A. (2013) Meta-analysis of association between obsessive-compulsive disorder and the 3′ region of neuronal glutamate transporter gene SLC1A1. *Am. J. Med. Genet., Part B 162B*, 367−79.
(33) Horiuchi, Y., Iida, S., Koga, M., Ishiguro, H., Iijima, Y., Inada, T., Watanabe, Y., Someya, T., Ujike, H., Iwata, N., Ozaki, N., Kunugi, H., Tochigi, M., Itokawa, M., Arai, M., Niizato, K., Iritani, S., Kakita, A., Takahashi, H., Nawa, H., and Arinami, T. (2012) Association of SNPs linked to increased expression of SLC1A1 with schizophrenia. *Am. J. Med. Genet., Part B 159B*, 30−7.
(34) Afshari, P., Myles-Worsley, M., Cohen, O. S., Tiobech, J., Faraone, S. V., Byerley, W., and Middleton, F. A. (2015) Characterization of a Novel Mutation in SLC1A1 Associated with Schizophrenia. *Mol. Neuropsychiatry 1*, 125−44.
(35) Hansen, K. B., Yi, F., Perszyk, R. E., Menniti, F. S., and Traynelis, S. F. (2017) NMDA Receptors in the Central Nervous System. *Methods Mol. Biol. 1677*, 1−80.
(36) Menniti, F. S., Lindsley, C. W., Conn, P. J., Pandit, J., Zagouras, P., and Volkmann, R. A. (2013) Allosteric modulators for the treatment of schizophrenia: targeting glutamatergic networks. *Curr. Top. Med. Chem. 13*, 26−54.
(37) Arriza, J. L., Fairman, W. A., Wadiche, J. I., Murdoch, G. H., Kavanaugh, M. P., and Amara, S. G. (1994) Functional comparisons of three glutamate transporter subtypes cloned from human motor cortex. *J. Neurosci. 14*, 5559−69.


DOI: 10.1021/acschemneuro.9b00447
*ACS Chem. Neurosci.* XXXX, XXX, XXX−XXX

(38) Dunlop, J., McIlvain, H. B., Carrick, T. A., Jow, B., Lu, Q., Kowal, D., Lin, S., Greenfield, A., Grosanu, C., Fan, K., Petroski, R., Williams, J., Foster, A., and Butera, J. (2005) Characterization of novel aryl-ether, biaryl, and fluorene aspartic acid and diaminopropionic acid analogs as potent inhibitors of the high-affinity glutamate transporter EAAT2. *Mol. Pharmacol. 68*, 974−82.
(39) Jensen, A. A., and Bräuner-Osborne, H. (2004) Pharmacological characterization of human excitatory amino acid transporters EAAT1, EAAT2 and EAAT3 in a fluorescence-based membrane potential assay. *Biochem. Pharmacol. 67*, 2115−2127.
(40) Sagot, E., Jensen, A. A., Pickering, D. S., Pu, X., Umberti, M., Stensbol, T. B., Nielsen, B., Assaf, Z., Aboab, B., Bolte, J., Gefflaut, T., and Bunch, L. (2008) Chemo-enzymatic synthesis of (2S,4R)-2-amino-4-(3-(2,2-diphenylethylamino)-3-oxopropyl)pentanedioic acid: a novel selective inhibitor of human excitatory amino acid transporter subtype 2. *J. Med. Chem. 51*, 4085−92.
(41) Esslinger, C. S., Agarwal, S., Gerdes, J., Wilson, P. A., Davis, E. S., Awes, A. N., O'Brien, E., Mavencamp, T., Koch, H. P., Poulsen, D. J., Rhoderick, J. F., Chamberlin, A. R., Kavanaugh, M. P., and Bridges, R. J. (2005) The substituted aspartate analogue L-beta-threo-benzyl-aspartate preferentially inhibits the neuronal excitatory amino acid transporter EAAT3. *Neuropharmacology 49*, 850−61.
(42) Hansen, J. C., Bjørn-Yoshimoto, W. E., Bisballe, N., Nielsen, B., Jensen, A. A., and Bunch, L. (2016) beta-Sulfonamido Functionalized Aspartate Analogues as Excitatory Amino Acid Transporter Inhibitors: Distinct Subtype Selectivity Profiles Arising from Subtle Structural Differences. *J. Med. Chem. 59*, 8771−8786.
(43) Jensen, A. A., Erichsen, M. N., Nielsen, C. W., Stensbol, T. B., Kehler, J., and Bunch, L. (2009) Discovery of the first selective inhibitor of excitatory amino acid transporter subtype 1. *J. Med. Chem. 52*, 912−5.
(44) Erichsen, M. N., Huynh, T. H., Abrahamsen, B., Bastlund, J. F., Bundgaard, C., Monrad, O., Bekker-Jensen, A., Nielsen, C. W., Frydenvang, K., Jensen, A. A., and Bunch, L. (2010) Structure-activity relationship study of first selective inhibitor of excitatory amino acid transporter subtype 1:2-Amino-4-(4-methoxyphenyl)-7-(naphthalen-1-yl)-5-oxo-5,6,7,8-tetrahydro-4H-chrom ene-3-carbonitrile (UCPH-101). *J. Med. Chem. 53*, 7180−91.
(45) Hansen, S. W., Erichsen, M. N., Fu, B., Bjørn-Yoshimoto, W. E., Abrahamsen, B., Hansen, J. C., Jensen, A. A., and Bunch, L. (2016) Identification of a New Class of Selective Excitatory Amino Acid Transporter Subtype 1 (EAAT1) Inhibitors Followed by a Structure-Activity Relationship Study. *J. Med. Chem. 59*, 8757−8770.
(46) Madsen, C., Jensen, A. A., Liljefors, T., Kristiansen, U., Nielsen, B., Hansen, C. P., Larsen, M., Ebert, B., Bang-Andersen, B., Krogsgaard-Larsen, P., and Frolund, B. (2007) 5-Substituted imidazole-4-acetic acid analogues: synthesis, modeling, and pharmacological characterization of a series of novel gamma-aminobutyric acid(C) receptor agonists. *J. Med. Chem. 50*, 4147−61.
(47) Fu, H., Zhang, J., Tepper, P. G., Bunch, L., Jensen, A. A., and Poelarends, G. J. (2018) Chemoenzymatic Synthesis and Pharmacological Characterization of Functionalized Aspartate Analogues As Novel Excitatory Amino Acid Transporter Inhibitors. *J. Med. Chem. 61*, 7741−7753.
(48) Vidyacharan, S., Shinde, A. H., Satpathi, B., and Sharada, D. S. (2014) A facile protocol for the synthesis of 3-aminoimidazo-fused heterocycles via the Groebke−Blackburn−Bienayme reaction under catalyst-free and solvent-free conditions. *Green Chem. 16*, 1168−1175.
(49) Rostamnia, S., and Hassankhani, A. (2013) RuCl3-catalyzed solvent-free Ugi-type Groebke−Blackburn synthesis of aminoimidazole heterocycles. *RSC Adv. 3*, 18626−18629.
(50) Rousseau, A. L., Matlaba, P., and Parkinson, C. J. (2007) Multicomponent synthesis of imidazo[1,2-a]pyridines using catalytic zinc chloride. *Tetrahedron Lett. 48*, 4079−4082.
(51) Varma, R. S., and Kumar, D. (1999) Microwave-accelerated three-component condensation reaction on clay: solvent-free synthesis of imidazo[1,2-a] annulated pyridines, pyrazines and pyrimidines. *Tetrahedron Lett. 40*, 7665−7669.
(52) Hansen, S. W., Erichsen, M. N., Fu, B., Bjorn-Yoshimoto, W. E., Abrahamsen, B., Hansen, J. C., Jensen, A. A., and Bunch, L. (2016) Identification of a New Class of Selective Excitatory Amino Acid Transporter Subtype 1 (EAAT1) Inhibitors Followed by a Structure-Activity Relationship Study. *J. Med. Chem. 59*, 8757.
(53) Rigby, J. H., and Laurent, S. (1998) Addition of Alkyl and Aryl Isocyanides to Benzyne. *J. Org. Chem. 63*, 6742−6744.


DOI: 10.1021/acschemneuro.9b00447
*ACS Chem. Neurosci.* XXXX, XXX, XXX−XXX